DEPARTMENT OF NATIONAL RESOURCES

BUREAU OF MINERAL RESOURCES, GEOLOGY AND GEOPHYSICS

Record 1977/41

Southern Cooper Basin Magneto-telluric Survey, South Australia, 1974

by

R.F. Moore, D.W. Kerr, K. Vozoff and D.L.B. Jupp

Record 1977/41

Southern Cooper Basin Magneto-telluric Survey, South Australia, 1974

by

*R.F. Moore, *D.W. Kerr, **K. Vozoff and

***D.L.B. Jupp

* Bureau of Mineral Resources

** Macquarie University

*** Macquarie University now at Comm. Scientific and Industrial Research Organisation (CSIRO)

CONTENTS

		Page
	SUMMARY	
1.	INTRODUCTION	1
	1.1 Acknowledgments	2
2.	GEOLOGY	2
	2.1 Regional geology	2
	2.2 Stratigraphy	2
3.	PREVIOUS GEOPHYSICS	4
	3.1 Aeromagnetics	4
	3.2 Gravity	5
	3.3 Seismic	7
4.	PRESURVEY MODELLING	8
	4.1 Introduction	8
	4.2 The response of individual well models	9
	4.3 The response of the average formation resistivity model	12
	4.4 Conclusions from modelling	14
5.	FIELD SURVEY OBJECTIVES AND PROGRAM	15
	5.1 Objectives	15
	5.2 Proposed program	16
	5.3 Actual program	16
6.	DATA RECORDING	16
7.	DATA PROCESSING AND PRESENTATION	18
	7.1 Processing	18
	7.2 Presentation, data selection, and data quality	18
8.	INTERPRETATION	20
9.	CONCLUSIONS	24
10.	REFERENCES	27
	APPENDIX 1 : MTCALC (1-dimensional MT modelling)	
	APPENDIX 2 : Operational data, staffing, and equipment	2
	APPENDIX 3 : Sample processing output.	

TABLE OF FIGURES

Figure 1 : Australian Sedimentary Basins

Figure 2 : Major Structural Elements, Southern Cooper Basin

Figure 3 : Locality Map showing Well Sections

Figure 4 : Schematic Resistivity Interpretation Section A-B

Figure 5 : Schematic Resistivity Interpretation Section C-D

Figure 6 : Magneto-Telluric Sites

Figure 7 : Gidgealpa A Apparent Resistivity XY

Figure 8 : Gidgealpa A Apparent Resistivity YX

Figure 9 : Gidgealpa A Phase XY

Figure 10 : Gidgealpa A Phase YX

Figure 11 : Gidgealpa A Rotation Angle

Figure 12 : Interpretation (1D) - Moomba A

Figure 13 : Interpretation (1D) - Moomba B

Figure 14 : Interpretation (1D) - Moomba C

Figure 15 : Interpretation (1D) - Gidgealpa A

Figure 16 : Interpretation (1D) - Gidgealpa B

Figure 17 : Horizontally Layered Inversion Models

Figure 18 : Geological Section

Figure 19 : Magnetic Tipper Data

Figure 20 : Magnetic Tipper Data

Figure 21 : Model which would produce Tipper Data

Figure 22 : Comparison between predicted and acquired data

TABLE OF PLATES

Plate 1 : Bouguer Gravity

Plate 2 : "C" Horizon Isopach

Plate 3 : "P" Horizon Isopach

Plate 4 : "Z" Horizon Isopach

TABLES

Table 1 : Cooper Basin Generalized Stratigraphy

Table 2 : Stratigraphy of the Recent-Tertiary Sediments

Table 3 : Calculated Curves for Well Models

Table 4 : Average Formation Resistivities

Table 5 : Data Recorded

Table 6 : Tabulated Interpreted Results

SUMMARY

The Cooper Basin is a Permo-Triassic intracratonic infrabasin lying beneath the Mesozoic Great Artesian Basin. Large proven reserves of natural gas make the Cooper one of the most economically important onshore basins in Australia. The Permian (Gidgealpa Group) formations serve as both source and reservoir in the producing areas. Low porosity rather than structure, however, is generally the main factor influencing the accumulation of hydrocarbons; hence, any exploration technique that might yield information about porosity, either directly or indirectly, is of considerable importance. As the bulk formation resistivity (the inverse of conductivity) of in-situ sedimentary rocks is directly related to the porosity of the rocks themselves, and since the magneto-telluric (MT) method gives information about the resistivity of the rocks encountered beneath a recording site, then the MT method might help to better define the location and extent of hydrocarbon accumulations. One of the authors (Moore) carried out extensive evaluation and interpretation of geophysical data from the Cooper Basin in 1973 to 1974 (Moore 1975); interpretation included the derivation of electrical models from smoothed well-log data. A decision was made by BMR to use the extensive information available in the Cooper Basin as a check on the reliability of field MT data in Australia by directly comparing MT field data with MT data produced from well-log models.

For the above reasons, an MT survey was conducted in the Cooper Basin in South Australia during the period August to September, 1974. One of the primary aims of the survey was to map porosity (indirectly). A secondary aim was to map the economic (sedimentary) basement and investigate the possibility of pre-Permian reservoirs in the older sedimentary sequences underlying the Cooper Basin. Deep drilling had intersected porous limestones below the Permian. The survey was undertaken jointly by BMR and Macquarie University. Five stations were occupied and more than 150 data files (normally 2048 points/file) were recorded. Site locations were dictated by access as

floodwaters covered the major part of the area and roads were not usable beyond the immediate vicinity of the Moomba and Gidgealpa fields.

Although most of the on-site time was devoted to recording, some processing (scalar Cagniard resistivities and phases only) was carried out in the field. Full processing yielding tensor impedance, tipper information, and rotation data was completed after returning to Canberra. Two component rotated apparent resistivity and phase plots were then produced. Differences between the two curves at each site were not sufficient to define smooth tensor rotation angles at any site and imply that the area must be remarkably uniform laterally in the vicinity of the test sites.

Data quality was generally good although scattered in the 0.1-1.0 second period decade. This was subsequently established to be due to noise in the Geotronics equipment and power supply hum induction.

By a technique commonly referred to as "numerical inversion", horizontally-layered models were fitted to the averaged data from each of the five sites; the isotropic nature of the data enabled horizontally-layered models to be used. Several conclusions can be drawn from these resultant models and the tipper data despite the fact that site coverage was not extensive enough to permit more positive interpretation. The stratigraphy of the Great Artesian Basin is mappable using the magneto-telluric method. However, porosity changes within the Gidgealpa Group were too small to be discernible. The boundary between the Permian and the underlying sediments is not apparent owing to poor resistivity contrasts at the contact. No major porous zones exist beneath the Permian horizons at any of the five sites. More extensive measurements might, however, observe deep conductive zones such as that drilled in Kalladeina No. 1.

Unexpectedly large variations in the vertical magnetic field were observed at quite large lateral distances (ten kilometres) from the Gidgealpa

and Big Lake structures and it was possible to locate the strike directions of these quite accurately ($\pm$5 degrees). The ability of the MT technique to locate such structure at considerable lateral distances is important for widely spaced reconnaissance work.

1. INTRODUCTION

Reconnaissance gravity and seismic surveys in southwestern Queensland and northeastern South Australia during 1957 led to the discovery of the Cooper Basin and to the drilling of Delhi-Frome-Santos Innamincka No. 1 well in 1959. Subsequent seismic and drilling activity by the Delhi-Santos Group (Delhi International Oil Corporation and Santos Limited) led to the definition of the Permo-Triassic sedimentary sequence now known as the Cooper Basin (see Figure 1).

The Cooper Basin is a subsurface sedimentary basin about 30 000 square miles in area and extends northeastwards from Lake Blanche over 300 miles into southwestern Queensland. It has an average width of about 100 miles. The basin has no surface expression and Permian sediments are not exposed at the surface. Physiographically, the axis of the basin is reflected by Cooper Creek.

Exploration work responsible for the discovery of significant hydrocarbon accumulations in the basin consisted of geological surface investigations, airborne magnetometer, and extensive seismic and gravity surveys. Eight dry holes were drilled before the drilling of Gidgealpa No. 2 and the discovery of the Gidgealpa gas field in late 1963.

To date, over 130 wells have been drilled and of these approximately 40 percent have realised significant quantities of hydrocarbons. Fifteen oil and gas fields have been recognised. Two of these, namely Gidgealpa and Moomba, have supplied the Adelaide market since 1969. In 1973, the total reserve gas estimate alone was over 100 billion cubic metres (Beddoes, 1972).

The Cooper Basin is situated within some of the most arid parts of the Australian continent. Average rainfall is less than 182 mm and summer shade temperatures commonly reach 49°C. The country is extremely flat and extensively covered by north-trending linear desert dunes, interspersed with

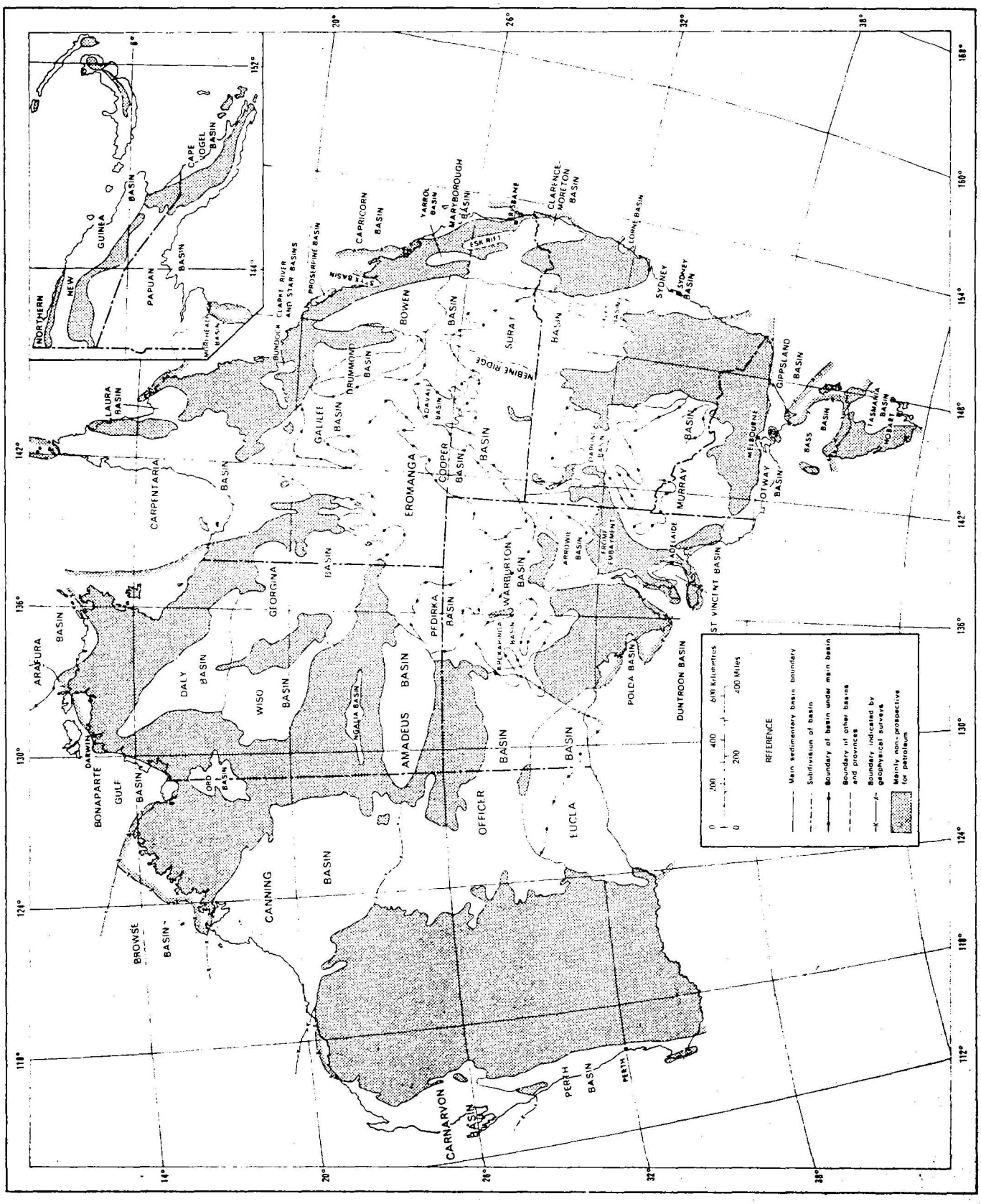

Figure 1 AUSTRALIAN SEDIMENTARY BASINS

clay pans and flood flats of Cooper Creek. Generally, Cooper Creek only flows water between April and July but owing to very heavy rains in Queensland and South Australia in 1974, a very large proportion of the land surface of the basin was covered by floodwaters at the time of this survey.

1.2 Acknowledgements

The assistance of the Australian Research Grants Commission (ARGC) and Macquarie University in providing funds for a large proportion of the logistic support used in the survey and the computer interpretation is gratefully acknowledged.

The cooperation of Delhi-Santos Pty Ltd was of great assistance to the planning and execution of the survey.

2. GEOLOGY

2.1 Regional geology

The Cooper Basin is a Permo-Triassic, intracratonic, miogeosynclinal infrabasin lying beneath the Great Artesian Basin. It unconformably overlies Lower Palaeozoic rocks folded in very late Devonian time. To the east, it is bounded by the Canaway Ridge, to the south by a basement ridge running from Naryilco to Kopperamanna, and to the west and north by an uplifted trend extending from Warbreccan to Kopperamanna. A description of the depositional history of the Cooper Basin can be found in Moore (1975).

2.2 Stratigraphy

A generalised stratigraphic chart is shown for the Cooper Basin in Table 1 (after Beddoes 1972). Table 2 (after Wopfner, 1966) shows detailed stratigraphy for the Recent-Tertiary sediments. Detailed descriptions of age, type section, stratigraphic position, and lithology for each of the stratigraphic units shown in Table 1 can be found in Moore (1975).

Table 1

COOPER BASIN

GENERALIZED STRATIGRAPHY

(after Beddoes, 1972)

SYSTEM	SERIES	STAGE	FORMATION (MAXIMUM THICKNESS IN METRES)	REMARKS and HYDROCARBONS
QUATERNARY and TERTIARY			UNNAMED	
				Disconformity
CRETACEOUS	UPPER	CENOMANIAN	WINTON FM.	
	LOWER	ALBIAN	TAMBO FM.	
		APTIAN	ROMA FM.	~~~ C-HORIZON
		NEOCOMIAN	TRANSITION BEDS	
JURASSIC	UPPER		MOOGA FM.	
	MIDDLE		BIRKHEAD FM.	
	LOWER		HUTTON SS.	
				Unconformity
TRIASSIC	MIDDLE TO LOWER		NAPPAMERRI FM. (495m)	TRIASSIC AND PERMIAN SEDIMENTS ARE NON-MARINE (Fluviatile, Deltaic, Flood-Plain, Poludal and Lacustrine)
PERMIAN	UPPER	TARTARIAN	GIDGEALPA GROUP: TOOLACHEE FM. (158m)	☼ Big Lake, Burke, Coonatie, Della, Epsilon, Gidgealpa, Moomba, Moorari, Mudrangie Strezelecki.
		KAZANIAN		
	LOWER	KUNGURIAN		
				Disconformity
		ARTINSKIAN	DARALINGIE BEDS (95m)	
			ROSENEATH SH. (81m)	
			EPSILON FM. (90m)	☼ Gidgealpa, Epsilon.
			MURTEREE SH (79m)	☼ Fly Lake. ☼ Big Lake, Bralga, Brumby, Burke, Daralingie, Epsilon, Fly Lake,
			PATCHAWARRA FM. (610m)	☼ Gidgealpa, Moomba, Moorari, Mudrangie, Packsaddle, Roseneath,
			MOORARI BEDS	☼ Tirrawarra, Toolachee. ☼ Fly Lake, Moorari.
		ARTINSKIAN TO SAKMARIAN	TIRRAWARRA SS. (122m)	○ Fly Lake, Moorari, Tirrawarra.
				Unconformity ?
		SAKMARIAN	MERRIMELIA FM. (396m)	PERIGLACIAL
CARBONIFEROUS			? ? ? GRANITE INTRUSIVE	
				Unconformity
DEVONIAN			"INNAMINCKA RED BEDS"	
				Unconformity
ORDOVICIAN			UNNAMED	
				Unconformity
CAMBRIAN			UNNAMED	
				Unconformity
PRECAMBRIAN			UNNAMED	

OLD TERMS: UPPER MBR — MIDDLE MBR — LOWER MBR

Permian terminology after Gatehouse (1972)

11

TABLE 2. STRATIGRAPHY OF THE RECENT-TERTIARY SEDIMENTS IN THE SOUTHERN COOPER BASIN. Dashed lines between rock-units denote the uncertain position of a time-boundary.

Age	Rock Unit	Lithology
Quaternary	————	Gravel, silt and aeolian sand.
Pliocene	Etadunna Formation	White marly dolomite and dolmitic clay.
		UNCONFORMITY
Miocene	Silcrete Duricrust	Fossil soil profile, consisting of bleached kaolinitic zone capped by dense quartz-silcrete.

	No Deposition	
Eocene	Unnamed	Coarse, freshwater sands, grey to yellow, lignite clays, highly polished conglomerate at base.
		DISCONFORMITY

Turonian?	Mt Howie Sandstone	White, torrentially bedded sandstone.
		DISCONFORMITY
Cretaceous	Winton Formation	As previously described.

3. PREVIOUS GEOPHYSICS

As mentioned previously, the Cooper Basin has no surface expression and Permo-Triassic sediments are not exposed at the surface. Both these factors thus dictated the use of geophysical methods and subsequent drilling to define the structure of the sediments in the basin.

The aeromagnetic method first illustrated the extent and thickness of the sedimentary section in the basin. However, the magnetic basement has not yet been equated with any particular horizon in the type section intersected in wells. As a result, the interpretation of depths to basement are somewhat suspect. Reconnaissance gravity data, on the other hand, outlined the limits of the basin and made it possible to site detailed gravity and seismic surveys.

The major structural elements of the basin are readily discernible on the Bouguer gravity maps and many local structures are apparent. Seismic reflection profiling, however, contributed more to an understanding of the subsurface geology than any other technique. Accurate depth calculations, verified by drilling, were made.

3.1 Aeromagnetic

The completion of several aeromagnetic surveys led to a nearly complete picture of the broadscale magnetic features of the southwestern Great Artesian Basin overlying the Cooper Basin. These surveys were undertaken by Aero Services Corporation for Delhi/Australian Petroleum Limited (Aero Services Corp, 1962) and Oilmin (Milton & Morony, 1973), by the Bureau of Mineral Resources (see Aero Services Corp., 1962), and by Adastra-Hunting. These data were used to compile several comprehensive aeromagnetic maps which were interpreted.

Aero Service Corporation compiled and interpreted the major part of the data in 1962 and Compagnie Generale de Geophysique reinterpreted it in 1963 when more drilling and seismic data became available (see Laherrere & Drayton, 1965). It was found that the average of both interpretations agreed with the seismic data better than the individual interpretations.

The South Australian Department of Mines (Milton & Morony, 1973) subsequently compiled a 1:1 000 000 aeromagnetic map; several regional features are apparent. Contours of magnetic basement show several structural features which were subsequently proved by seismic techniques and drilling. These are the ridges to the northwest (the Birdsville Track Ridge) and to the south which control the limits of the Permian sedimentation, and the southwest trending anticlinal crests of the Innamincka and Gidgealpa structures (see Figure 2).

Two closed basinal areas are also delineated in the map. The first is north of and parallel to the Nappamerri Trough and the second coincides with the southwestern end of the Tenaperra Trough (see Figure 2). Quantitative interpretation of magnetic data is generally thought unreliable, however, as maximum computed depths to magnetic basement are typically of the order of 4000 metres, but in many areas wells drilled to depths in excess of this figure do not penetrate any horizon which can be positively identified as magnetic basement.

3.2 Gravity

The gravity method was used extensively in delineating gross and small-scale structural features in the Cooper Basin. Several reconnaissance (e.g. the Strzelecki Creek and Lake Gregory helicopter survey, 1965 (Lonsdale & Ingall (1965)) and detailed (e.g. southwest Cooper Basin gravity survey, 1968 (Delhi Australian Petroleum Limited, 1968) surveys were conducted but

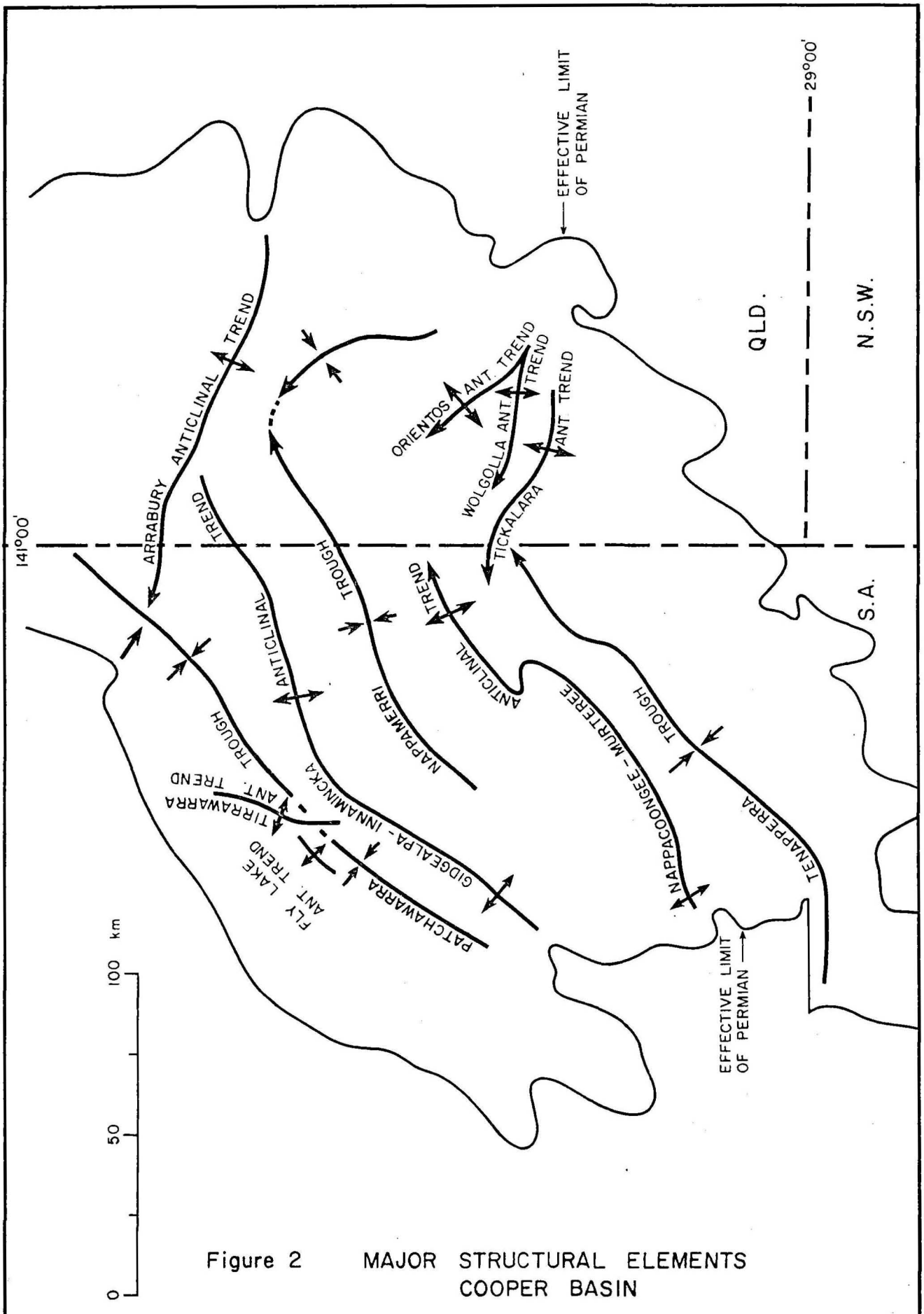

Figure 2 MAJOR STRUCTURAL ELEMENTS COOPER BASIN

it has become normal practice to carry out joint seismic and gravity surveys. Plate 1, taken from the southern Cooper Basin seismic and gravity survey report (Delhi Australian Petroleum Limited, 1969), shows Bouguer gravity data for that part of the Cooper Basin that contains the Gidgealpa and Moomba fields and the magneto-telluric (MT) survey area. A detailed discussion of the geological significance of this map can be found in the above survey report. Only a few of the more important features will be discussed here.

A quick perusal of the gravity contour map shows a profusion of gravity anomalies, large and small, both in areal size and in gravity relief. There appear to be no prominent regional trends dominating the entire map although there are several very large anomalies, large enough to be classed as regional features. The most prominent of these runs from the centre of the plate to the northeast corner and is a manifestation of the Nappamerri Trough (see Figure 2). A second feature can be seen crossing the northwest corner of the map and trending northeast. The origin of this feature is unknown but it has been suggested (Delhi Australian Petroleum Limited, 1969) that it may represent a sharp boundary between two large masses of adjacent rocks of different densities within the basement complex.

Together with these regional features there are over 30 local gravity highs, all of which are of such size, shape, and magnitude that they could be due to geological anomalies within the sedimentary section which might be of interest for hydrocarbon exploration. Many of them coincide with associated anomalies in the seismic contours over the mapped area where the gravity and seismic surveys overlap. Note the strong anomaly centred on the Gidgealpa structure and the associated northeast-trending anomalies which are an expression of the Gidgealpa-Innamincka Anticlinal Trend (see Figure 2). Another group of nine anomalies also trending northeast marks the location of the Nappacoongee-Murteree Anticlinal Trend.

3.3 Seismic

Extensive seismic reflection and refraction surveys were conducted in the Cooper Basin. The basic objectives were twofold: (1) to detect and map large structural traps in areas of relatively thick sequences of sedimentary rocks in order that wildcat locations could be made with optimum chances of success, and (2) to increase the general geological knowledge of the region. These surveys were necessitated by the fact that Tertiary and Recent sediments nearly everywhere conceal all the Mesozoic and older rocks and rarely reflect underlying structure.

Mesozoic sediments, down to the Lower Jurassic Hutton Sandstone (see Table 1), are remarkably uniform in thickness and lithology throughout the region. Their involvement in tectonic events is minor compared with that of older rocks, and they are readily observable and mappable by seismic methods. The very strong "C" horizon (see Plate 2) is drawn from a reflecting band associated with sediments at the top of the Lower Cretaceous Transition Beds.

The Permian, of greatest significance economically, is usually readily mappable. The top of these strata is mapped by a regionally continuous, strong "P" seismic event (see Plate 3) which originates from interbedded coals, shales and sands at the top of the Permian Gidgealpa Group. This horizon grades into the "Z" horizon when the Permian is absent. The "Z" horizon (see Plate 4) marks the base of the Permian (where present) or Triassic sediments, a regional angular unconformity on which Permo-Carboniferous and older rocks subcrop. This reflection band is not persistent owing probably to the variable lithology in the pre-Permian section. Where reflections are weak, questionable correlations and projections of dip have often been used to establish continuity. However, coupled with well control and the existing subsurface data, the mapping of the "Z" horizon is considered reasonably reliable.

Many of the regional structural features of the basin (see Figure 2) can be seen in all three isopach maps (Plates 2-4). The Gidgealpa-Innamincka Anticlinal Trend is the most striking of these features, and it can be seen to cut across the entire area in a northeast direction. The Gidgealpa, Merrimelia, and Innamincka structures all fall on this line. To the northwest, the Patchawarra Trough is apparent as a fairly broad, relatively shallow-dipping depression. This feature is cut by the Tirrawarra Anticlinal Trend.

To the south, the Nappamerri Trough is seen as a very extensive topographically flat area on which the Daralingie and the producing Moomba structures are superimposed. This trough is bounded to the south by the Nappacoongee-Murteree Anticlinal Trend, a feature well marked on the "C" isopach, but becoming less apparent on the "P" and "Z" isopachs. The Murteree, Nappacoongie, and Dullingari structures lie along this trend. The Tenappera Trough, which is not obvious to the south, is apparent to the east.

There are, however, several notable differences from horizon to horizon, two of which are discussed here. Firstly, dips on the major features increase noticeably from the "C" horizon to the "P" horizon, and from the "P" horizon to the "Z" horizon, the latter being more pronounced. The rapid thinning of Permian sediments is again illustrated. Secondly, structural complexity and faulting increases rapidly from the "C" to the "Z" isopach, illustrating the degree of structural deformation to which the pre-Permian sediments have been subjected.

4. PRESURVEY MODELLING

4.1 Introduction

The electrical responses of geological structures can be modelled by sophisticated numerical models. Sedimentary basins, being usually regarded as relatively simple, can be represented by simple one-dimensional

models. These models are made up of infinitely extending, horizontal layers of constant resistivity (i.e. homogeneous and isotropic) and finite thickness, except for the bottom-most layer which is a half-space. Each layer is equivalent to a stratigraphic unit or group of units where the difference in resistivity between adjacent units is not significant. Given such a model, it is possible to predict the response of the geological structure (in this case, a sedimentary basin) to the MT method. The outcome of an MT survey might then be anticipated. This was done before the start of field work in the Cooper Basin by Moore (1975).

4.2 The Responses of individual well models

In the Cooper Basin, the only way the variation of resistivity with depth can be defined from pre-existing information is by quantitatively interpreting the electrical wireline logs available from the extensive logging programs conducted in wells within the basin. Accurate determination of un-invaded formation resistivities (Rt) can be made using these tools. Three devices in particular were used. They were the ES lateral, the IES (6FF40), and the laterolog (LL7 and DLL). The ES lateral device was the most commonly used log. Corrections to interpreted apparent resistivity values were made, where appropriate, for borehole diameter and drilling fluid resistivity. In all, 16 wells were interpreted (see Figure 3). Their choice was dictated mainly by the availability of usable logs for the total section penetrated in the well.

The final models for each of the wells are shown as resistivity-depth sections and are shown in Figures 4 and 5. The response of the geological section intersected in each of the wells (represented by the 16 layered models) was then calculated. The results, namely apparent resistivity and phase as a function of period, are shown in Table 3. Several qualitative conclusions can be drawn from these data.

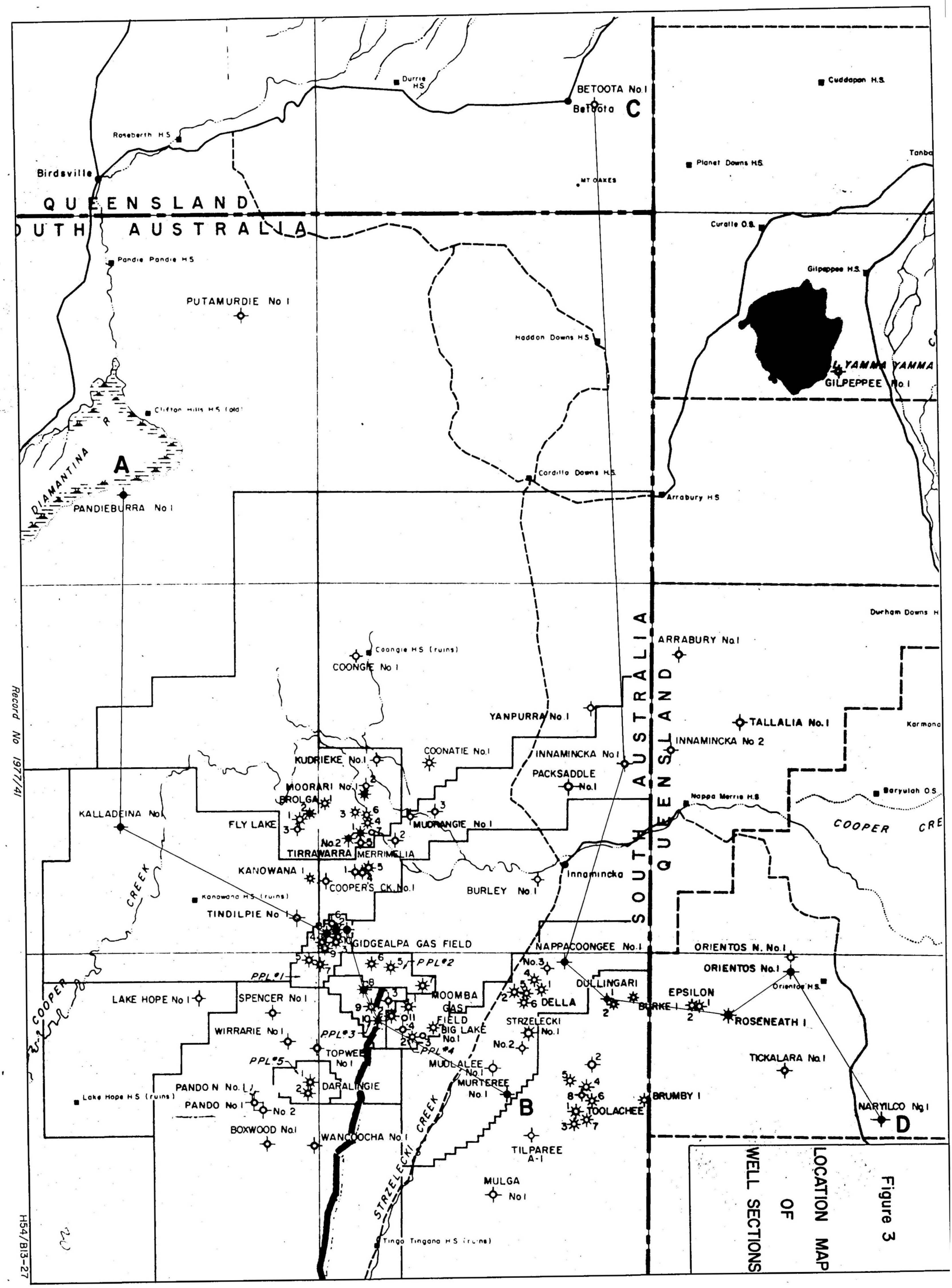

Figure 3 LOCATION MAP OF WELL SECTIONS

Record No 1977/41

H54/BI3-27

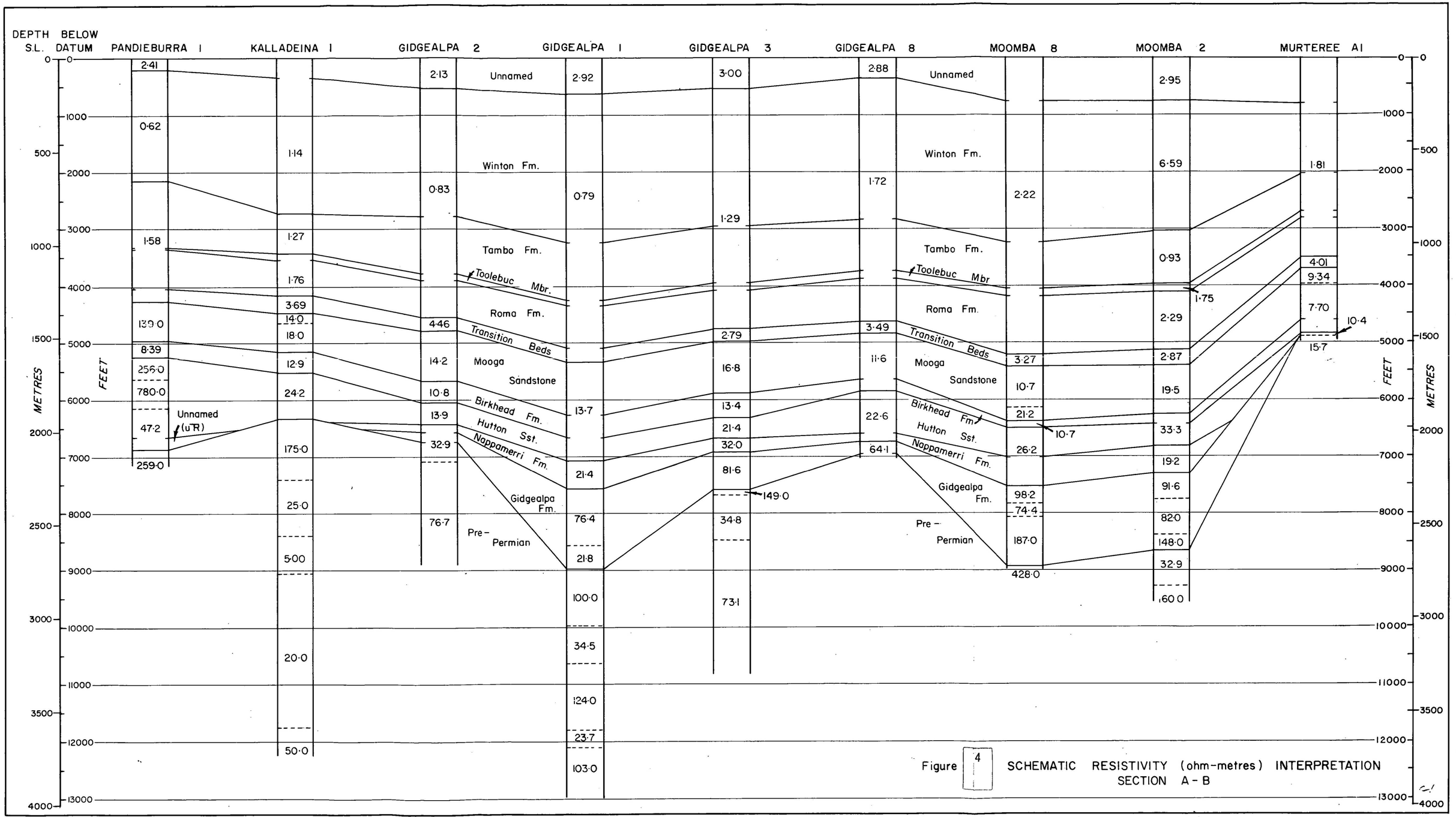

Figure 4 SCHEMATIC RESISTIVITY (ohm-metres) INTERPRETATION SECTION A - B

Based on H54/B13-10

Record No. 1977/41

H54/B 13-2

DEPTH BELOW S.L. | DATUM | BETOOTA | INNAMINCKA | NAPPACOONGIE | DULLINGARI | ROSENEATH | ORIENTOS | NARYILCO

METRES | FEET

Unnamed

Winton Fm.

Tambo Fm.

Toolebuc Mbr.

Roma Fm.

Transition Beds

Mooga Sandstone

Birkhead Fm.

Hutton Sst.

Nappamerri Fm.

Gidgealpa Fm.

Pre – Permian

BETOOTA	INNAMINCKA	NAPPACOONGIE	DULLINGARI	ROSENEATH	ORIENTOS	NARYILCO
1·32	1·82	1·50	3·65	2·00	2·26	1·68
3·92					2·74	5·23
12·5	4·43	3·48	5·31	4·00	4·54	1·51
31·5	23·2	9·72	17·6	10·0	13·9	1·83
	5·37				24·6	84·2
	14·7		13·2	25·0		102·0
	24·4	20·8	17·8		42·1	686·0
57·0	34·4	25·7	30·2	60·0	53·7	
	44·8	90·5	118·0		77·9	
	32·8		62·3			
	16·5	432·0			288·0	
78·5			103·0			
148·0		336·0				
96·1			492·0			

Figure 5 SCHEMATIC RESISTIVITY (ohm-metres) INTERPRETATION SECTION C – D

Based on H54/B13–11

Record No. 1977/41

H54/B 13–1

At the short-period end (0.1 second), the apparent resistivity corresponds closely to the resistivity of the unnamed Recent-Tertiary sediments. The apparent resistivity then drops to less than 2 ohm-metres between 1 and 10 seconds, depending most likely on the thickness of the formations above the Transition Beds. Local anomalous variations in the upper section significantly affect some of the curves at these short periods. For example, in Moomba No. 2, the resistivity of the Winton Formation is unusually high, causing the response curve to be significantly different at these periods.

The response to individual formations below the Transition Beds is not apparent. The apparent resistivity curves rise at approximately 45 degrees to the period axis, to a value of between 10 and 100 ohm-metres at about a period of 300 seconds. From this point, it asymtotically approaches the half-space resistivity.

TABLE 3. The calculated curves for the 16 well models (Sections A-B and C-D) are tabulated here. For the tabulated data, each of the wells is represented by the following numbers:

1	Pandieburra No. 1
2	Kalladeina No. 1
3	Gidgealpa No. 2
4	Gidgealpa No. 1
5	Gidgealpa No. 3
6	Gidgealpa No. 8
7	Moomba No. 8
8	Moomba No. 2
9	Murteree A-1
10	Betoota No. 1
11	Innamincka No. 1
12	Nappacoongie No. 1
13	Dullingari No. 1
14	Roseneath No. 1
15	Orientos No. 1
16	Naryilco No. 1

A more detailed description of the method used to calculate these data can be found in Appendix 1.

APPARENT RESISTIVITY

	WELLS:								
PERIOD	1	2	3	4	5	6	7	8	9
.1	1.6	1.4	2.1	3.0	2.9	2.7	2.2	2.8	1.8
.3	1.1	1.4	1.7	2.2	2.3	2.3	2.2	3.7	1.8
1.0	.9	1.4	1.3	1.5	1.9	2.1	2.2	4.2	1.7
3.2	.6	1.2	1.0	1.1	1.4	1.6	1.8	2.7	1.6
10.0	.8	1.5	.8	.8	1.4	2.0	2.4	3.0	2.4
31.6	1.9	3.0	1.5	1.2	2.8	4.2	5.8	6.4	4.2
100.0	5.2	6.7	3.6	2.8	6.5	9.2	15.4	15.2	6.9
316.2	13.8	13.3	8.6	7.0	14.0	18.0	33.3	32.5	9.6
1000.0	32.8	22.0	17.9	16.0	25.6	29.4	83.6	58.4	11.8
3162.3	66.7	30.8	30.9	31.0	38.9	40.6	152.4	87.6	13.4
10000.0	112.2	37.9	44.8	49.6	50.7	49.3	230.7	113.0	14.3
31622.8	158.4	42.7	56.3	67.2	59.4	55.3	288.3	131.3	14.9
100000.0	195.4	45.8	64.3	80.7	65.0	59.0	349.3	143.1	15.3
316227.8	220.8	47.6	69.5	88.8	68.4	61.2	381.6	150.2	15.4
1000000.0	238.7	48.6	72.5	95.3	70.4	62.4	401.2	154.4	15.6

PHASE

	WELLS:								
PERIOD	1	2	3	4	5	6	7	8	9
.1	57.2	45.0	50.2	52.0	50.9	49.2	45.0	41.6	45.0
.3	55.6	45.0	53.4	56.5	52.7	49.6	45.0	38.6	45.0
1.0	53.1	45.7	52.9	55.9	52.0	49.5	45.9	48.1	45.5
3.2	45.2	41.9	51.6	54.4	48.6	43.9	41.5	47.4	37.7
10.0	24.4	27.4	36.2	42.9	31.2	27.3	22.8	28.6	28.4
31.6	11.6	18.6	19.2	22.6	18.3	18.4	12.0	17.1	26.7
100.0	8.6	18.4	13.8	13.4	16.0	18.6	10.3	15.9	29.9
316.2	10.4	22.6	15.5	13.1	19.5	23.1	13.2	19.8	34.3
1000.0	14.9	28.5	20.6	17.1	25.3	29.0	18.6	25.7	38.1
3162.3	21.2	33.9	26.9	23.1	31.2	34.4	25.1	31.7	40.8
10000.0	27.8	38.1	32.8	29.5	36.2	38.4	31.3	36.5	42.5
31622.8	33.6	40.8	37.3	34.9	39.6	41.1	36.3	39.8	43.6
100000.0	37.9	42.6	40.4	38.8	41.8	42.7	39.7	42.0	44.2
316227.8	40.8	43.6	42.3	41.3	43.2	43.7	41.9	43.3	44.5
1000000.0	42.5	44.2	43.4	42.9	44.0	44.3	43.2	44.0	44.7

APPARENT RESISTIVITY

	WELLS:						
PERIOD	10	11	12	13	14	15	16
.1	1.3	1.8	1.5	3.6	2.0	2.2	1.9
.3	1.3	1.8	1.5	3.7	2.0	2.3	1.8
1.0	1.2	1.7	1.5	3.2	1.9	2.1	1.5
3.2	1.1	1.6	1.2	3.2	1.7	2.1	1.5
10.0	2.0	2.3	1.7	6.5	2.6	4.3	3.1
31.6	4.7	4.1	4.3	16.8	5.7	11.0	8.7
100.0	11.2	6.7	11.7	41.7	11.9	27.0	23.8
316.2	23.0	9.6	29.3	91.7	21.4	58.1	59.9
1000.0	39.5	12.1	64.2	169.2	32.3	104.9	131.4
3162.3	56.8	13.8	117.8	259.1	41.9	157.5	241.0
10000.0	71.0	14.9	178.3	339.3	48.9	203.2	366.6
31622.8	81.0	15.6	233.6	398.2	53.5	238.2	477.4
100000.0	87.2	16.0	273.2	436.6	56.2	257.5	553.2
316227.8	91.0	16.2	298.0	460.0	57.8	270.4	610.6
1000000.0	93.2	16.3	314.6	473.7	58.8	278.0	642.5

PHASE

	WELLS:						
PERIOD	10	11	12	13	14	15	16
.1	45.0	45.0	45.0	45.0	45.0	45.0	47.8
.3	45.0	45.0	45.0	45.2	45.0	44.1	46.8
1.0	46.0	45.7	46.1	45.3	46.0	43.9	46.5
3.2	34.5	38.9	38.7	30.4	37.6	30.2	29.9
10.0	19.1	28.7	20.8	15.7	23.4	16.0	13.6
31.6	14.0	26.2	11.1	11.5	18.4	12.0	8.3
100.0	15.8	29.0	9.9	13.3	20.6	14.0	8.9
316.2	20.9	33.5	12.9	18.3	25.8	19.1	12.5
1000.0	27.2	37.5	18.3	24.7	31.6	25.5	18.2
3162.3	33.0	40.4	24.9	30.9	36.3	31.6	24.8
10000.0	37.5	42.3	31.1	36.0	39.7	36.5	31.2
31622.8	40.5	43.4	36.1	39.5	41.9	39.8	36.2
100000.0	42.4	44.1	39.6	41.8	43.2	42.0	39.6
316227.8	43.5	44.5	41.8	43.1	44.0	43.3	41.8
1000000.0	44.1	44.7	43.2	43.9	44.4	44.0	43.2

4.3 The response of the average formation resistivity model

It was shown in the last section that the Cretaceous to Recent formations have a significant affect on the magnitude and shape of the response curves for each of the 16 well models. The affects of the older formations were, however, not apparent. A method of establishing the relative contributions of each of the formations is given below.

Using the data shown in Figures 4-5, a layered model was calculated by averaging the resistivity data for each of the 16 wells interpreted. Although this model represents only, at best, a first approximation, it can be seen that the average resistivities typify the variation of resistivity with depth.

The apparent resistivity measured over a horizontally layered Earth at a given frequency is a non-linear function of the constituent layer resistivities and thicknesses (see Appendix 1). If the partial derivatives of the apparent resistivity with respect to each of the model parameters were calculated, the magnitude of the partial derivatives would indicate at any given frequency the relative influence of each layer to the response curves. This was done not by calculating the partials directly but rather by varying a single model parameter (either a thickness or a resistivity) and observing the differences between the original and new response curves for the average formation resistivity model (Table 4).

TABLE 4. AVERAGE FORMATION RESISTIVITIES

	Average Thickness (ft)	No. of values used	Average Resistivity ohm-m
Recent-Tertiary	500	9	2.4
Winton	2000	17	2.0
Tambo	1000	16	1.7
Roma	1000	16	1.8
Transition Beds	300	16	3.4
Mooga Sandstone	800	18	18.0
Birkhead	250	15	13.0
Hutton Sandstone	400	13	20.0
Nappamerri	600	12	25.0
Gidgealpa Group	600	22	73.0

The relative responses of the constituent layers fell of rapidly with increasing depth from a maximum for layer 2 (Winton Formation equivalent) to a minimum for each of the layers below layer 5 (Transition Beds equivalent). It was found that the affect of layers 6-10 on the shape and magnitude of the response curve for the average resistivity model is minimal (see Moore, 1975). This implies that the formations lying beneath the Transition Beds (with the possible exception of the basal pre-Perlian) contribute little to the response curve; the Gidgealpa Group is undetectable if the average formation resistivity model is typical of the basin.

4.4 Conclusions from modelling

Several conclusions are drawn regarding the response of the formations encountered in the Cooper Basin and the application of the MT method. Firstly, the unnamed Recent-Tertiary sediments, the Winton, Tambo, and Roma Formations and, to some degree, the Transition Beds, mainly affect the response curves calculated for the Cooper Basin models. The method is suited to the mapping of these formations. The response of the economically important Gidgealpa Group, however, is not significant. The formations above and below this group do not act as markers as their response is either insignificant (Nappamerri Formation) or too variable (pre-Permian). This implies that the MT method would fail as an exploration tool used in the mapping of the Gidgealpa Group in the Cooper Basin if the values used to construct our models are representative. This is mainly due to poor resistivity contrasts and layer thicknesses within the lower parts of the section.

Secondly, the pre-Permian stratigraphy shows little or no significant response to the method, the only exception being in the interpreted well Kalladeina No. 1. It was hoped that the method might be used to map porosity in the pre-Permian. The pre-Permian geology is extremely variable lithologically and electrically, even in wells close to each other.

Thirdly, but more encouragingly, the method should prove useful in mapping gross resistivity changes in the true basement. Each of the wells used in the model study bottomed in the pre-Permian sediments, and seismic, gravity, and magnetic data have contributed little to an understanding of the nature of the basement. More significant resistivity contrasts are likely to exist between the pre-Permian sediments and the basement. As a result, a magneto-telluric survey should yield information about the nature of the basement and the deeper crust if sufficiently long periods are recorded.

In conclusion, it is emphasised that this study assumes infinitely extensive homogeneous horizontal layers. It does not consider possible large lateral resistivity variations such as from local changes within a layer, nor does it consider the often substantial affects of structural features. Such features can be modelled using 2-dimensional (and more recently 3-dimensional) techniques, but there were insufficient data and time in this case to do so.

5. FIELD SURVEY OBJECTIVES AND PROGRAM

5.1 Objectives

The specific objectives of the survey were as follows:

1. to ascertain whether or not the method is suited to mapping
   a) the thickness and lateral extent of the Gidgealpa Group, and
   b) changes in porosity within the Gidgealpa Group;
2. to map the structure of the pre-Permian economic basement and locate possible pre-Permian reservoirs previously undefined by seismic techniques owing to the three very strong reflectors higher up in the section; and
3. to obtain more information about the little-known true basement and lower crust.

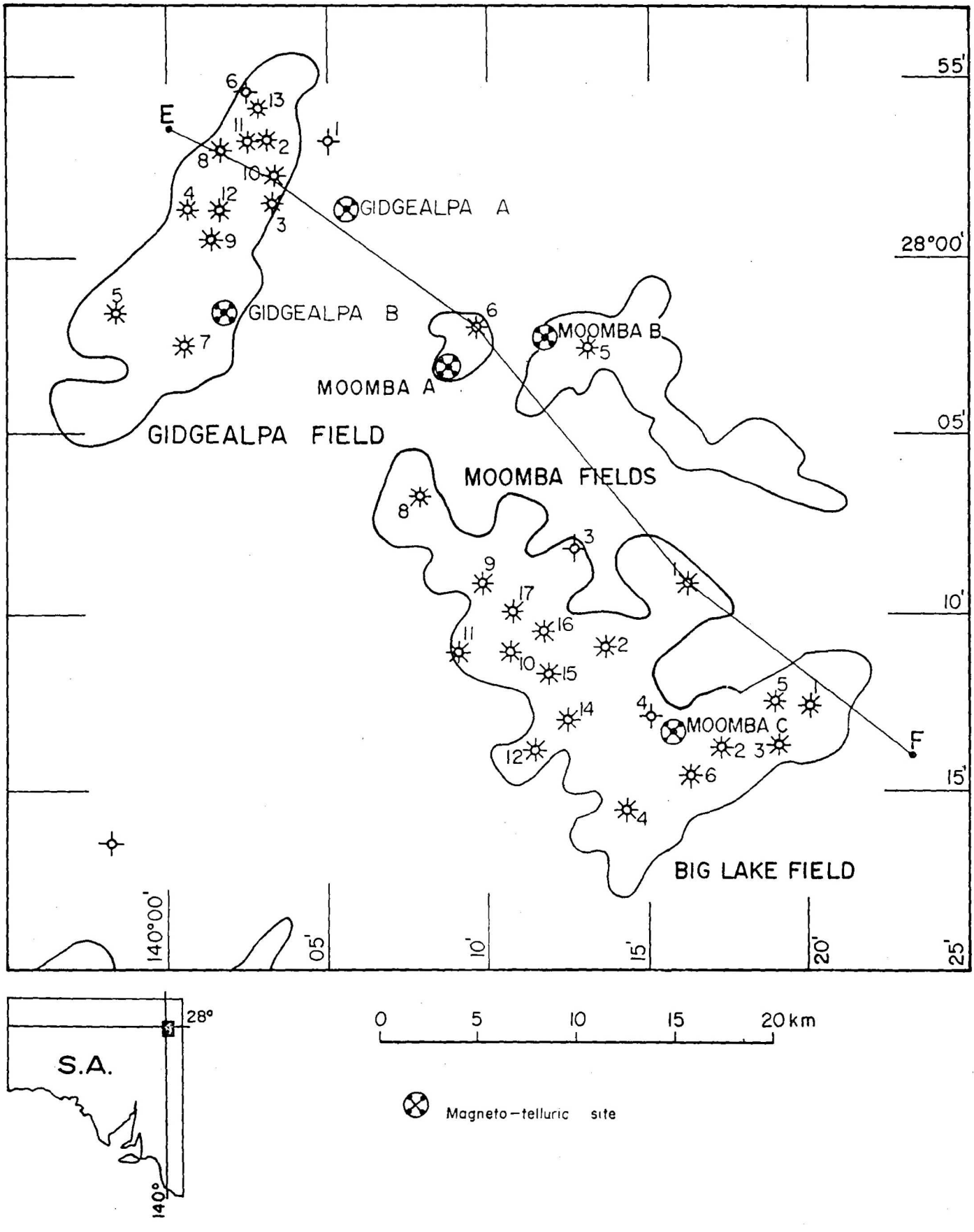

Figure 6 MAGNETO - TELLURIC SITES

5.2 Proposed program

The two sections (A-B, C-D) shown in Figure 3 were chosen as traverse lines so that field results could be tied in with the modelling previously done. Sites were to be occupied between Gidgealpa No. 8 and Moomba No. 2 on section A-B and between Nappacoongie No. 1 and Roseneath No. 1 on section C-D. Stations within the Gidgealpa and Moomba fields would be given priority. Stations along the section C-D would only be undertaken if time was available.

5.3 Actual program

The location and the number of stations were dictated by the two factors given below:

1. owing to very heavy rains in 1973 and 1974 in southwest Queensland and northeast South Australia, most of the Cooper Basin area was covered by flood waters; and
2. the time available for recording was severely shortened by vehicle and equipment breakdowns.

For these reasons, only 5 stations were recorded in the three weeks spent in the field. Three of these were located on the Moomba field (Moomba A, B and C) and two were recorded on the Gidgealpa field (Gidgealpa A and B). A list of recording times can be found in Appendix 2. The five recording sites are shown in Figure 6.

6. DATA RECORDING

A full description of site location and establishment, system configuration and recording procedures for magneto-telluric surveys can be found in Kerr, Moore & Spence (in prep.). The equipment used in the field was identical to the configuration used on the 1973 Murray Basin MT survey (Vozoff et al., 1975). Both Macquarie University and BMR took computer data

acquisition systems into the field but Macquarie's system developed a hardware fault and those data acquired by their system could not be used. The equipment is listed in Appendix 2 together with a block diagram for the system. This section deals only with the details of the actual data recorded in the Cooper Basin in 1974.

Data were recorded in the following frequency bands using the sampling intervals given:

Band	Frequency (hertz)	Sampling interval (ms)
1	10.0 - 256.0	5
2	10.0 - 25.0	5
3	1.0 - 25.0	10
4	0.1 - 2.0	100
5	0.01 - 0.125	1,100
6	0.002- 0.025	10,000
7	DC - 0.025	10,000

Between 26 and 39 data files of 2048 points on 5 channels (namely two electric and 3 magnetic components) were acquired for the 5 stations at which recording was done. Table 5 shows the number of data files recorded within the frequency bands given above.

TABLE 5. DATA RECORDED

Site	Band							Total
	1	2	3	4	5	6	7	
Moomba A	2	-	13	5	5	2	-	27
Moomba B	-	4	23	5	3	2	-	37
Moomba C	3	-	16	14	3	3	-	39
Gidgealpa A	-	-	11	9	3	3	-	26
Gidgealpa B	-	-	20	12	3	-	2	37

7. DATA PROCESSING AND PRESENTATION

7.1 Processing

At the conclusion of the Cooper Basin survey, comprehensive processing software was written for the BMR in-house HP2100 minicomputer system to allow computation of rotated tensor resistivities and full tipper analysis. Tensor resistivity software was written from the theory of Sims & Bostick (1969). Tipper analysis was based on the theory provided by Vozoff (1972) with some corrections to errors in the original text. The processing software is divided into two parts and may be run on either a stand-alone 16K word HP minicomputer with magnetic tape, or a 24K word disc-based minicomputer with magnetic tape. The processing software has since been successfully used on two later surveys in the field.

Of the 166 data files recorded in the Cooper Basin in 1974 approximately 10 percent were rejected owing to either noise introduced at the time of recording or signal saturation on one or more of the data channels. Hence approximately 150 data files were subsequently processed in Canberra on the Hewlett-Packard 2100 computer system. These data files included those previously processed in the field to yield scalar (Cagniard) resistivities and phases.

Unrotated and rotated impedance tensor data together with tipping vector (Tipper) analyses were output on a Gould 5000 printer/plotter. An example of the information that may be obtained from processing a single data file is shown in Appendix 3.

7.2 Presentation, data selection, and data quality

Apparent resistivities and phases for the two orthogonal components

of the rotated impedance tensor together with the rotation angles are normally plotted as a function of period (or frequency). Data selection is normally achieved by using two parameters, the degree of agreement between the predicted and actual components (i.e. coherency) and the tensor-skew. However, as band averaging and outlier rejection was to be applied to the data, only coarse coherency and skew cutoffs (0.76 and 1.0 respectively) were used to screen the data.

Plots of apparent resistivity and phase for both components together with tensor rotation angles for one site (namely Gidealpa A) are shown in Figures 7-11. Each plot shows a mean value plotted at the centre of the period band over which it was calculated and error bars represent plus or minus 1 standard deviation from the mean. Several qualitative conclusions can be drawn as regards data quality from these plots.

The range of useful data extends from 0.2 second (5 Hz) to 2000 seconds period. The data quality is not constant over this range, however. It is less reliable at both extremes as the number of points used to calculate the mean ("N" on the plots) is low. At least two noisy bands (large standard deviations imply more than background scatter) are also apparent. These are from 0.1 to 2.0 and from 100 to 200 seconds. These poor data were attributed to noise in the Geotronics equipment, namely chopper feed-through beating with the 50-Hz mains power supply (short period noise) and chopper offset drift (longer period noise).

The other four sites are similar to Gidgealpa A. The noticeable differences are that the above-mentioned noisy bands contain little data but Moomba A and Moomba C have useful data down to 0.05 second period (20 Hz).

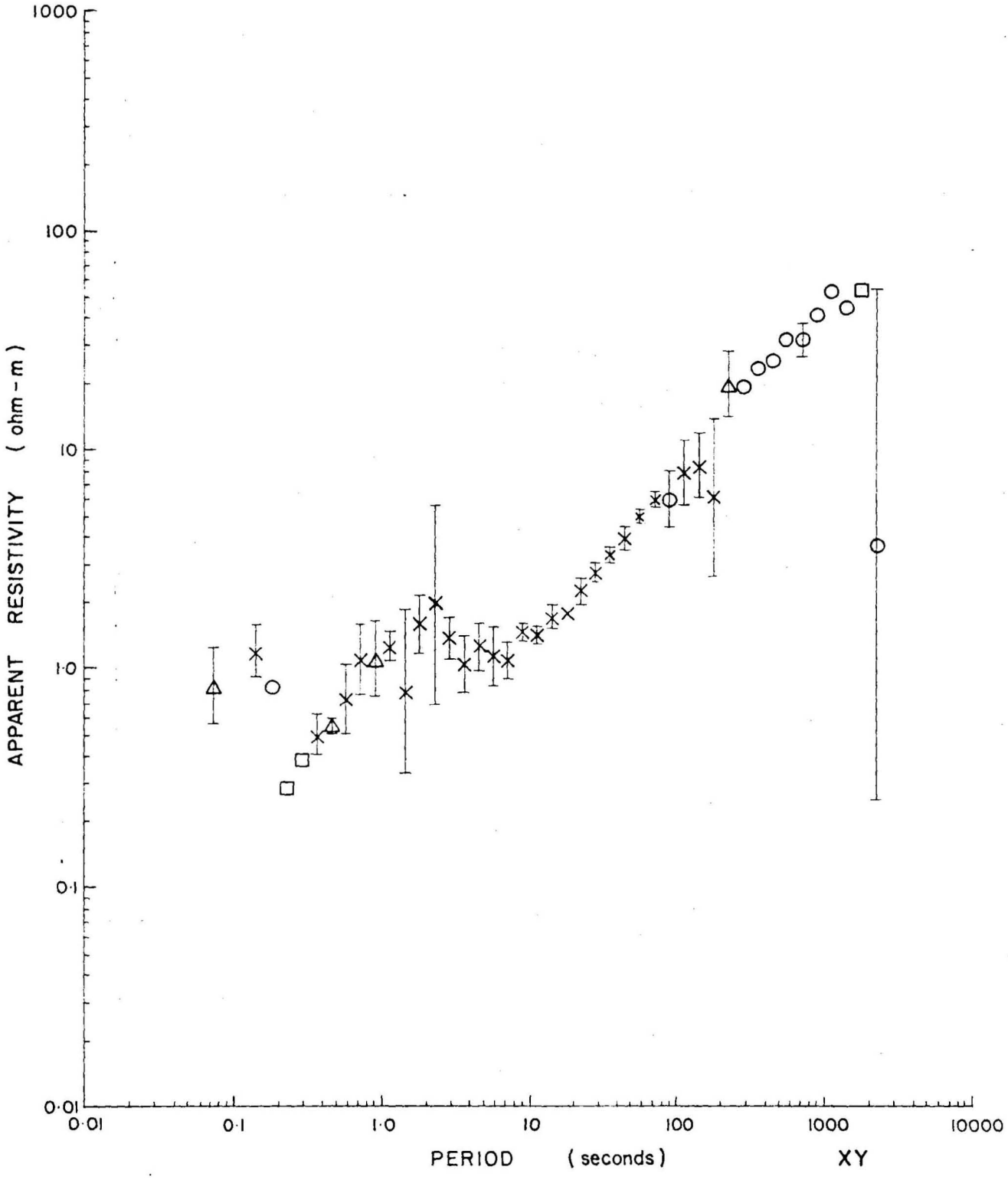

PERIOD	COH >	SKEW <
< 10	0·7	1·0
≥ 10	0·7	1·0

SYMBOLS

□ N = 1 △ N = 3

○ N = 2 × N > 3

Figure 7 COOPER BASIN MT : GIDGEALPA A

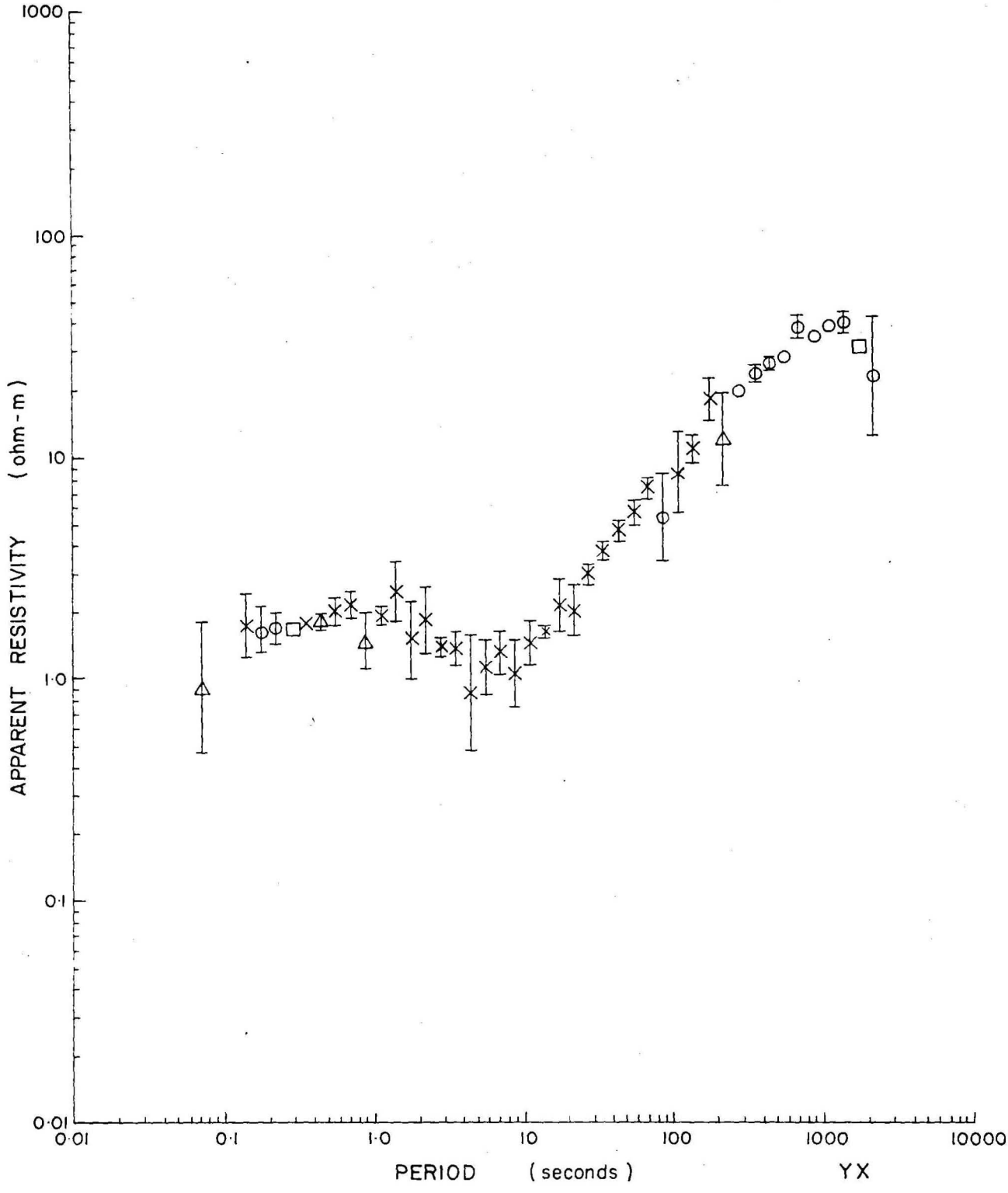

PERIOD	COH >	SKEW <	SYMBOLS	
< 10	0·7	1·0	□ N = 1	△ N = 3
≥ 10	0·7	1·0	○ N = 2	× N > 3

Figure 8 COOPER BASIN MT : GIDGEALPA A

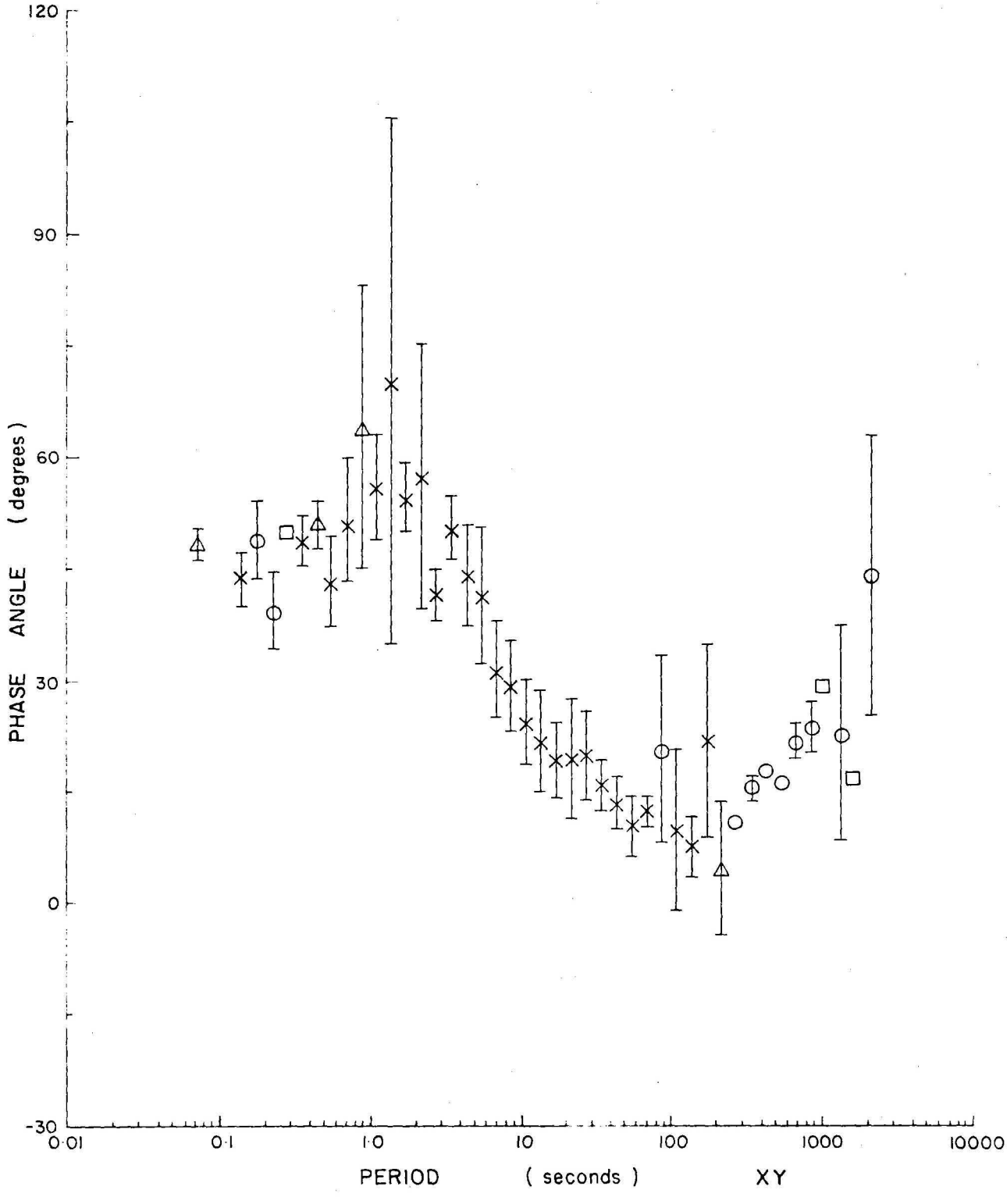

PERIOD	COH >	SKEW
< 10	0·7	1·0
≥ 10	0·7	1·0

SYMBOLS

□ N = 1 △ N = 3

○ N = 2 × N > 3

Figure 9 COOPER BASIN MT : GIDGEALPA A

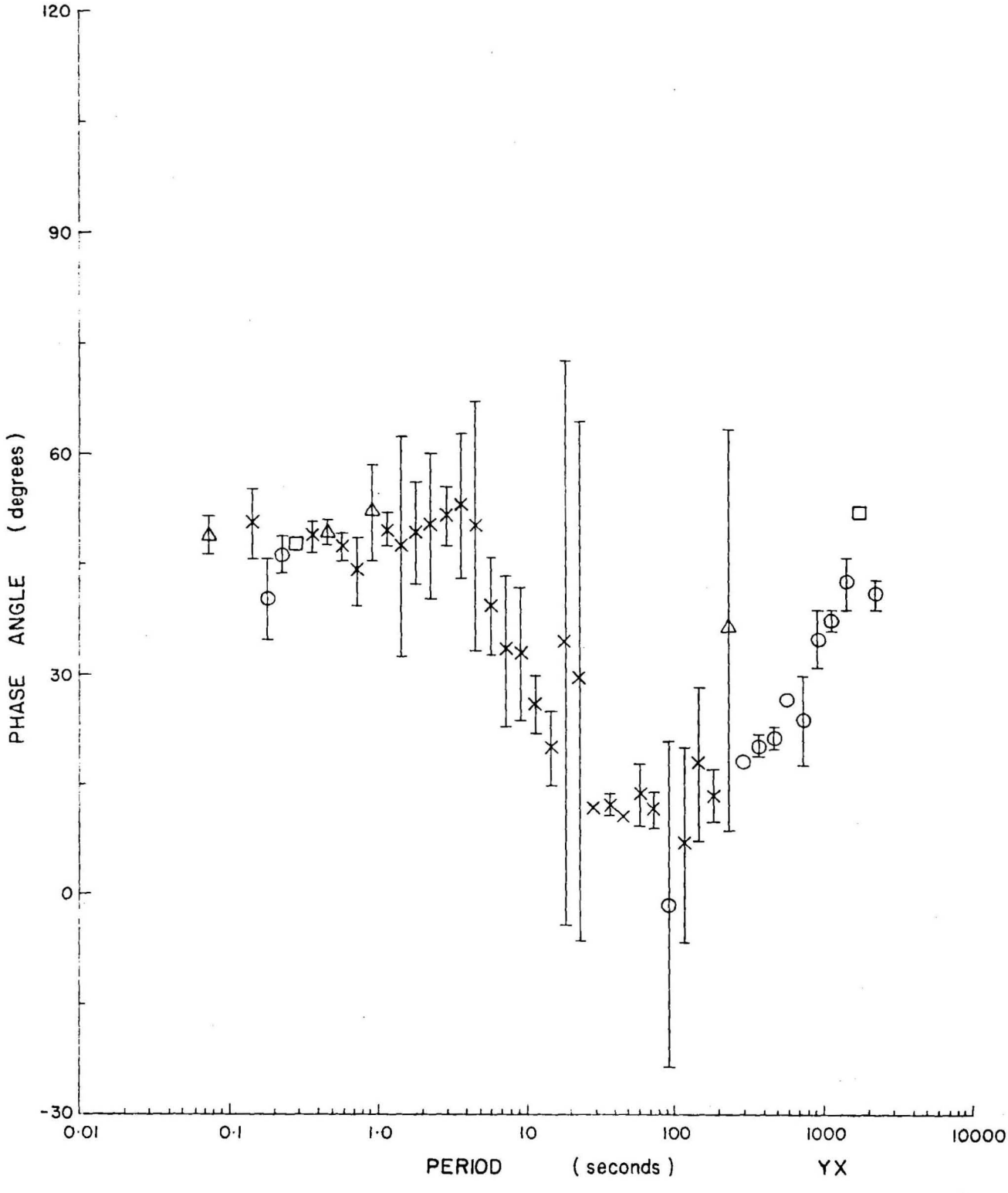

PERIOD	COH >	SKEW <
< 10	0·7	1·0
> 10	0·7	1·0

SYMBOLS

□ N = 1 △ N = 3

○ N = 2 × N > 3

Figure 10 COOPER BASIN MT : GIDGEALPA A

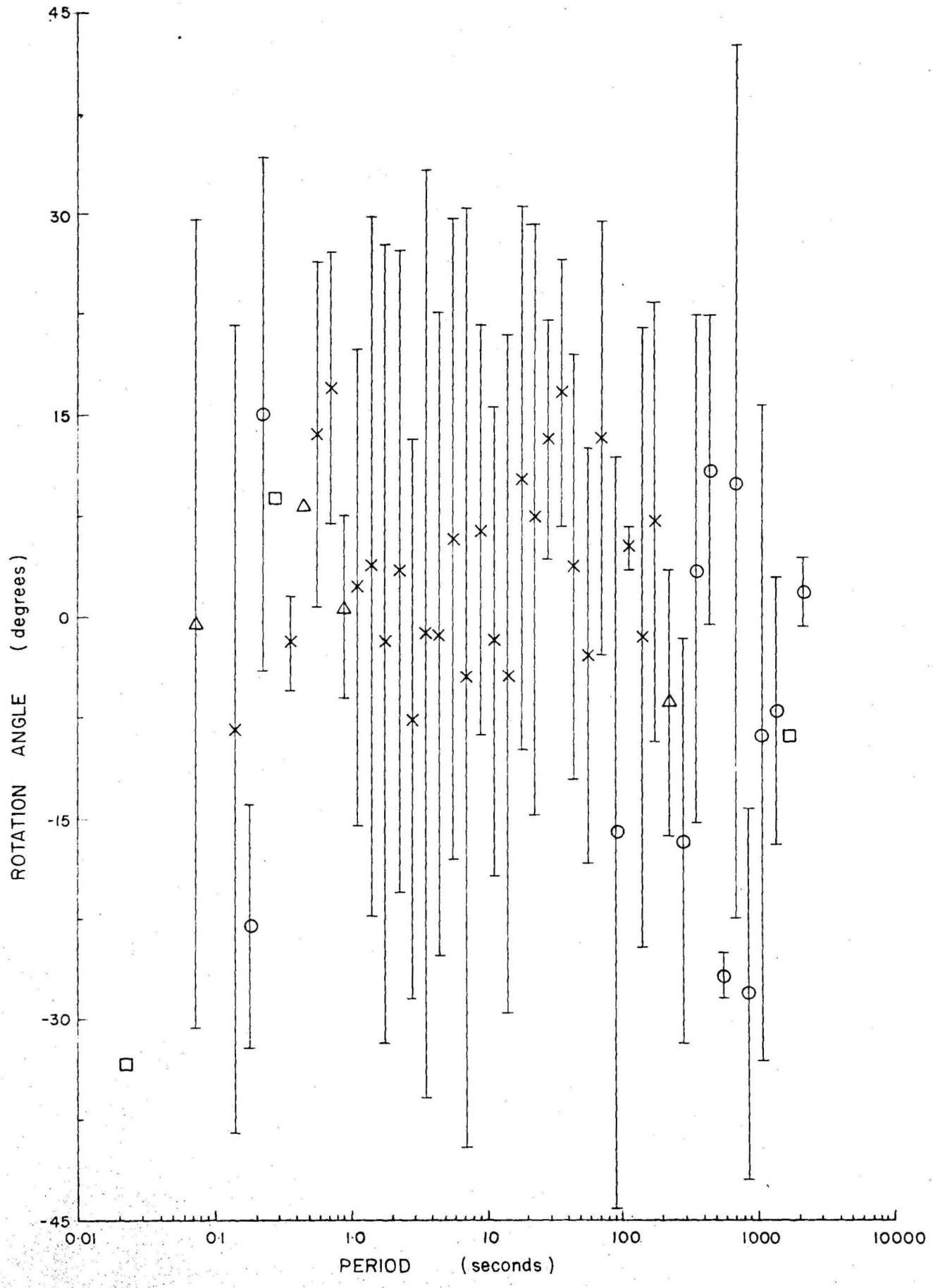

PERIOD	COH >	SKEW <
< 10	0·7	1·0
≥ 10	0·7	1·0

SYMBOLS

□ N = 1 △ N = 3

○ N = 2 × N > 3

Figure 11 COOPER BASIN MT : GIDGEALPA A

H54/B13-33

Record No. 1977/41

8. INTERPRETATION

Figures 12-16 show the two averaged apparent resistivity and phase components of the rotated tensors, calculated for each of the 5 sites and plotted against period. Differences between components and sites are very small except at the longest periods. Differences between components at each site were in fact not sufficient to define smooth tensor rotation angles. The area must be remarkably uniform laterally for this to occur. The task of distinguishing differences would not have been possible without computer inversion.

As already mentioned, the processed data have not been subjected to the usual acceptance criteria based on coherencies and skews. Rather, unscreened data were averaged into narrow frequency bands. Those of the original data values in each band which departed by more than two standard deviations from the band average were rejected as outliers, and the remaining data were re-averaged. It was still necessary to reject some points in the 0.1-1 second period decade because of scatter. This is a result of noise in the Geotronics equipment, the design of which is now being modified.

Moomba C data are very noisy owing to rapid drying near one porous pot electrode, and Gidgealpa B 12 phase data are poor, possibly for the same reason. No real evidence of noise due to the pipelines can be seen, but cathodic protection circuitry was switched off when we recorded in their vicinity.

The solid lines through each data set are layered model curves, obtained using the method of inversion (Jupp & Vozoff, 1975). The models are listed in Table 6, together with the probable range of each parameter. It will be observed that in most cases the curves do not fit the data points as closely as might be expected. This was also true of the earlier models fitted to the selected data values. The reason for this is believed to be the

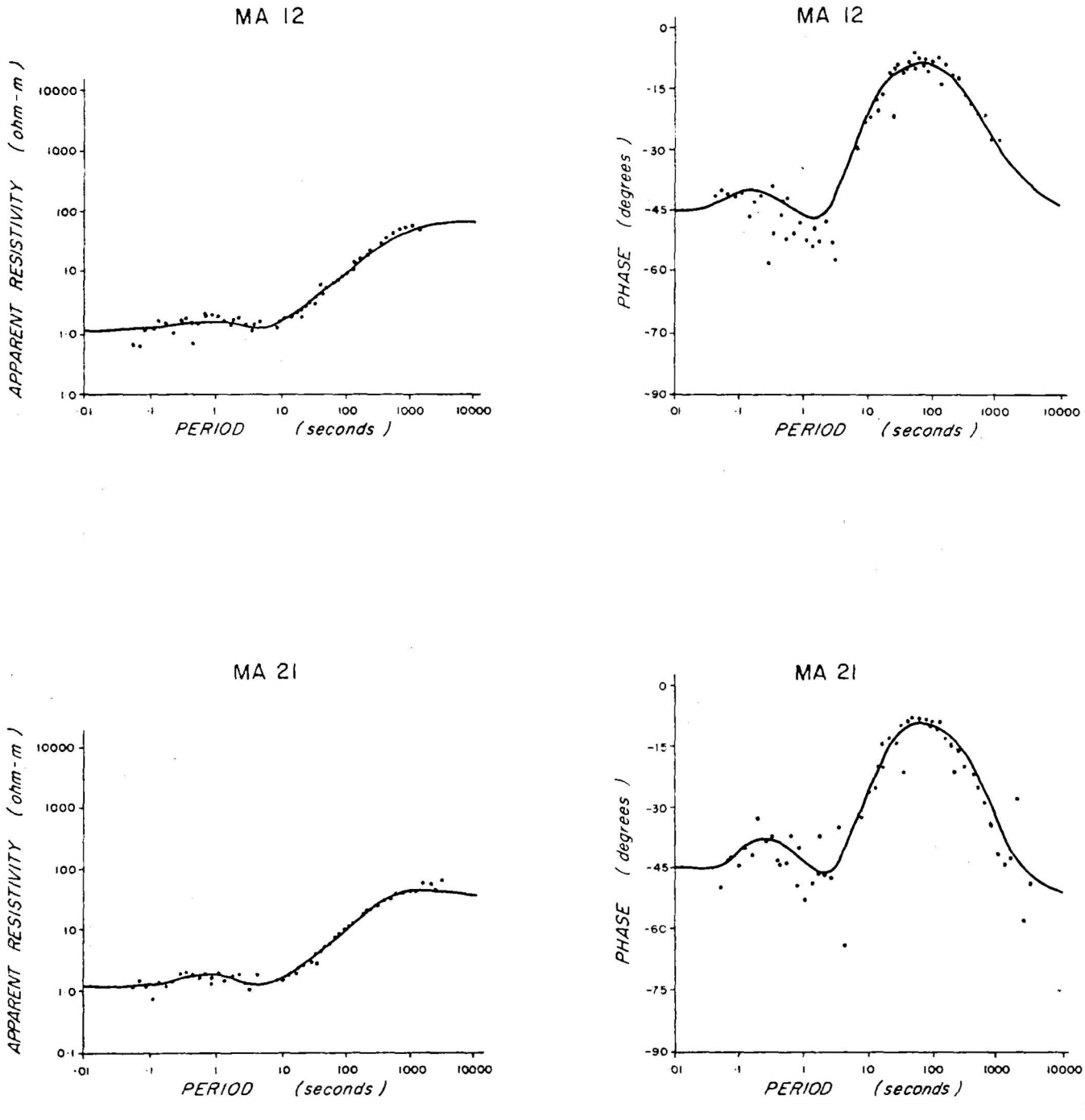

Figure 12 MOOMBA A ROTATED APPARENT RESISTIVITIES DERIVED FROM THE TENSOR ROTATED IMPEDANCE MATRIX AND ALLIED PHASE CURVES.

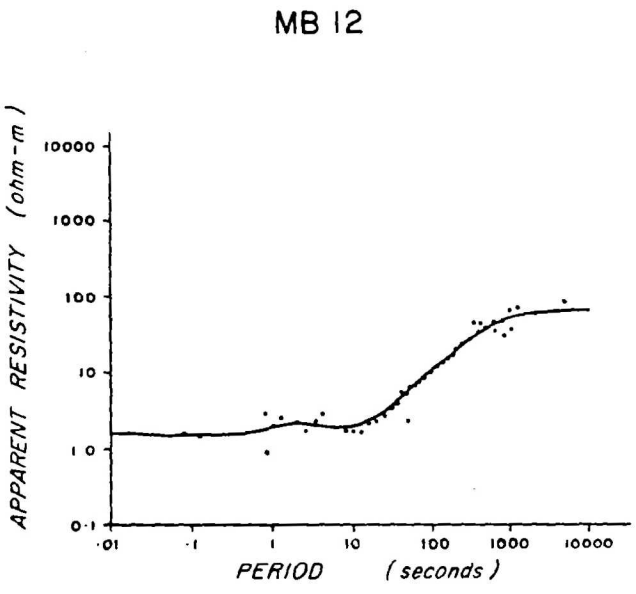

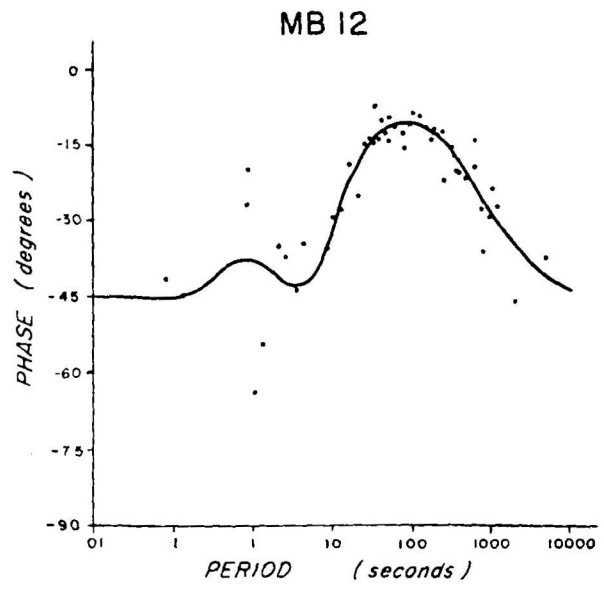

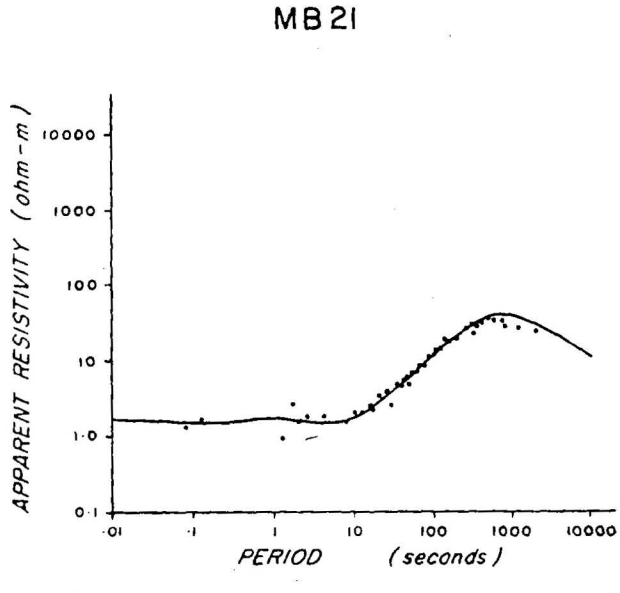

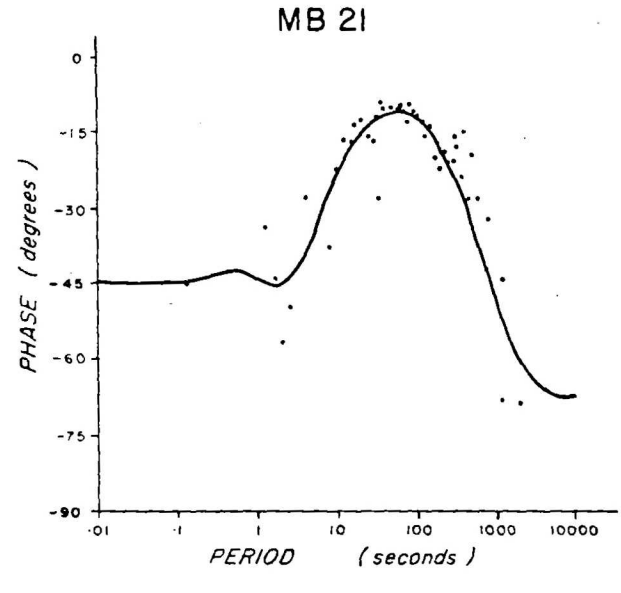

Figure 13 MOOMBA B ROTATED APPARENT RESISTIVITIES DERIVED FROM THE TENSOR ROTATED IMPEDANCE MATRIX AND ALLIED PHASE CURVES.

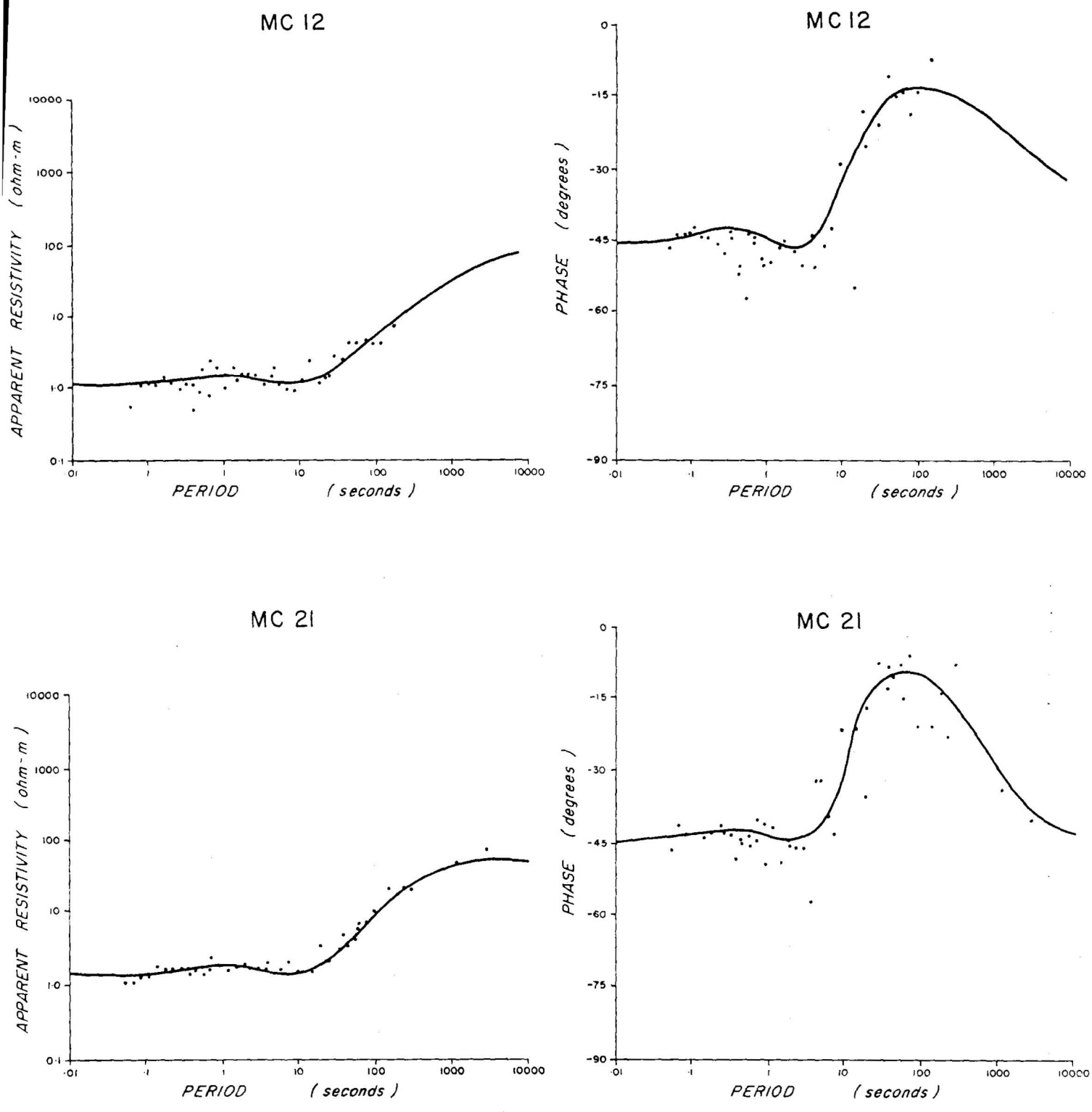

Figure 14 MOOMBA C ROTATED APPARENT RESISTIVITIES DERIVED FROM THE TENSOR ROTATED IMPEDANCE MATRIX AND ALLIED PHASE CURVES

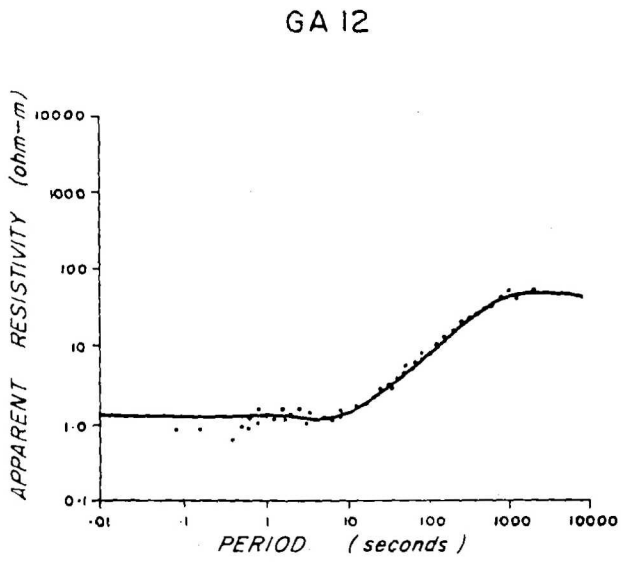

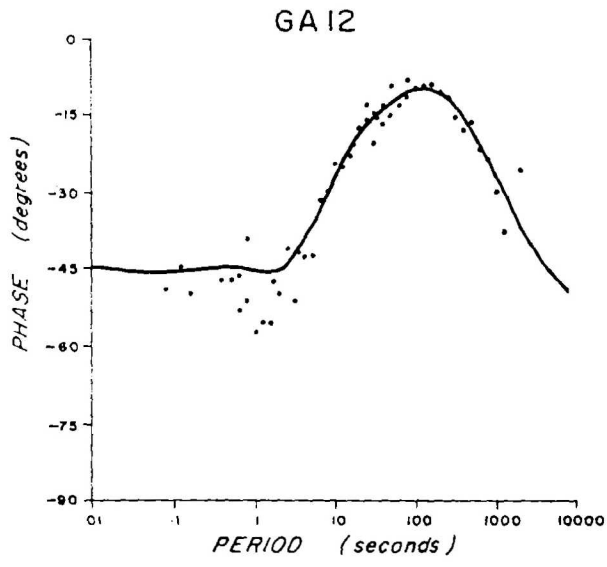

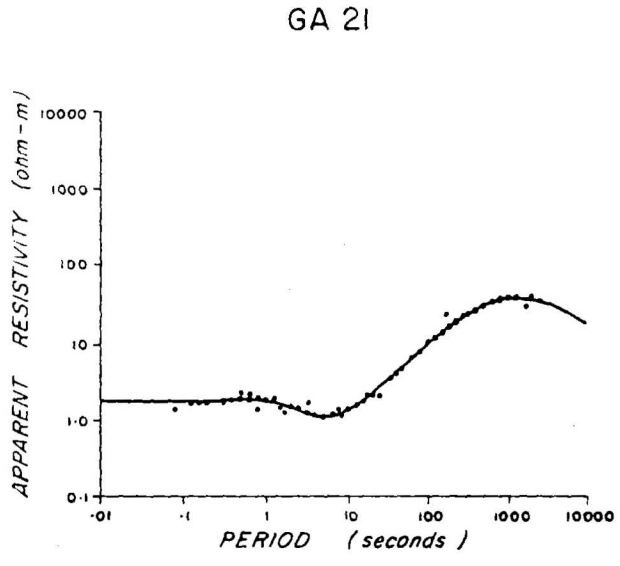

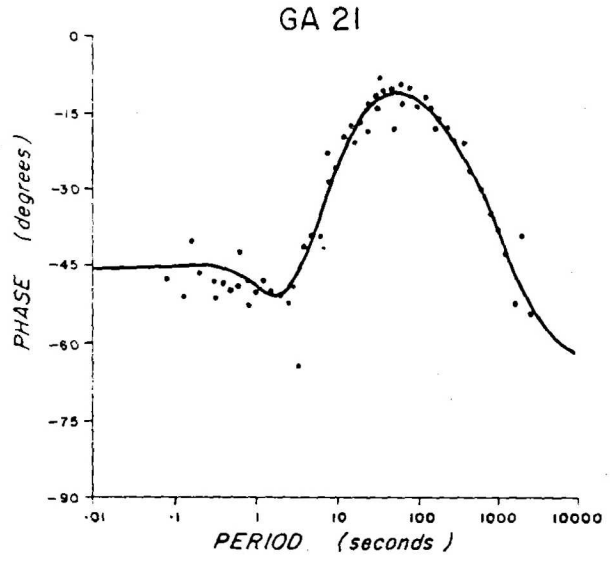

Figure 15 GIDGEALPA A ROTATED APPARENT RESISTIVITIES DERIVED FROM THE TENSOR ROTATED IMPEDANCE MATRIX AND ALLIED PHASE CURVES

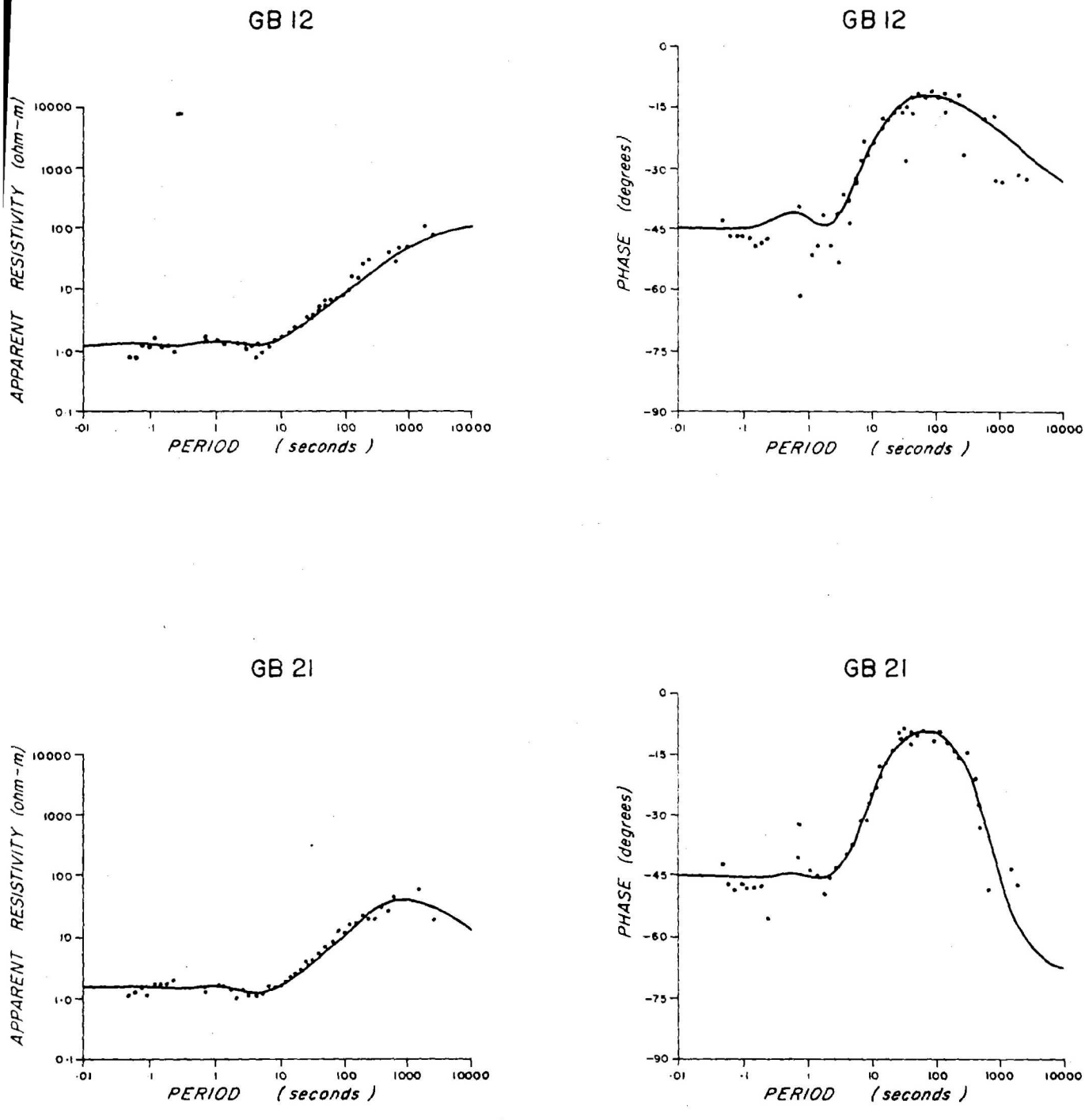

Figure 16 GIDGEALPA B ROTATED APPARENT RESISTIVITIES DERIVED FROM THE TENSOR ROTATED IMPEDANCE MATRIX AND ALLIED PHASE CURVES.

TABLE 6. TABULATED RESULTS - COOPER BASIN MT SURVEY - 1974

SITE	PARAMETERS				RANGES			
	P12		P21		P12		P21	
	P_i(-m)	Z_i(m)	P_i	Z_i	P_i	Z_i	P_i	Z_i
GIDGEALPA A	1.3	0	1.8	0	1.26-1.42	-	1.7-1.9	-
	1.4	500 U	.95	650	1.0 -2.0	U	.6-1.4	460-930
	1.5	880 U	2.3 U	1280	.8 -2.8	U	U	1200-1400
	115.	1510	1090.U	1500	70-180	1180-1900	U	1200-1900
	1300.U	37 km	32.	55 km	U	22-60 km	20-50	45-70 km
	26	126 km	4.5 T	120 km	15-50	105-150 km	(3-7)	100-150 k
GILDGEALPA B	1.2	0	1.4	0	1.12-1.18	-	1.38-1.49	-
	4.8 U	410	3.0 U	590	U	260-470	U	400-860
	.82 U	830	.90 U	850	U	730-950	U	650-1110
	750 U	1350	220	1320	U	1250-1450	170.-280	1160-1500
	200	33 kmU	1020 U	32 km T	150-270	U	U	(25.40 km
			2.2	99 km			1.4-3.4	90-110 k
MOOMBA A	1.3	0	1.4	0	1.2 - 1.4	-	1.26-1.46	-
	4.3 U	170	5.9 U	210	U	130-220	U	170-250
	1.3	340	1.4	440	1.1 -1.6	270-440	1.1 -1.8	340-560
	350.	1450	490.	1550	260-470	1300-1650	310-760	1320-1820
	57.	102 km	22	91 km	46-92	75-135 km	15-35	80-105 km
MOOMBA B	1.6	0	1.6	0	1.5 -1.7	-	1.5 -1.7	-
	4.2	350	3.5 U	420	3.1 -6.7	270-458	U	310-570
	1.7	1130	1.1 T	740	1.3 -2.1	990-1300	(.97-1.2)	580-930
	2200.U	2200	220.	1330	U	1950-2500	180-270	1170-1500
	66.	90 km	2.2	82 km	54-81	80-102 km	1.5 -3.1	77-88 km
MOOMBA C	1.2	0	1.6	0	1.1 -1.3	-	1.4 -1.7	-
	1.7	150	2.0	120.	1.4 -2.1	86-250	1.8 -2.1	60-230
	1.0	630	1.6	1300.	.6 -1.7	360-1100	1.1 -2.4	740-2300
	300.U	1400	2400.U	1800.	U	1100-1800	U	1500-2300
	120.	4900 U	55.	66 km	86-170	U	33-90	50-87 km

P_i : Layer i resistivity — P_i, P_i in -m

Z_i : Depth to top of i-th layer — Z_i, Z_i in m

Ranges: Strict error bounds for 1 precision level and assuming medium is horizontally layered.

U : Parameter is not resolved

( )T : Threshold parameter

following: These models were fitted to both apparent resistivities and phases together. By fitting on apparent resistivities alone, a much closer match was obtained to those points, but the phase fit was worse. When the same was done but weighting the phase fit more heavily, the apparent resistivity fit deteriorated. In the models shown, equal weights were placed on each.

This behaviour results because the region is not exactly horizontally layered. While it is possible to closely fit a layered mosel curve to either ρ_a or phase, the actual phase response corresponding to the observed ρ_a differs slightly from that of a truly horizontally layered medium.

The models of Table 6 are shown on a (split) linear depth scale in Figure 17. Their common features can be seen to be a region of low resistivity to about 1500 m, where there is a large increase. This corresponds to the rise at the Transition Beds observed by Moore (1975). Four of the sites show a decrease in resistivity, in at least one component, near 100 km. This feature was also observed in our 1973 survey 600 km to the southeast.

Small differences between components can be seen at each site at most depths. Those at Gigealpa B are due at least in part to the Gidgealpa structure, which extends to very shallow depths. Shallow differences shown at Gidgealpa A are probably not meaningful, while those at greater depths likely indicate lateral effects of the structure. Moomba A appears to be isotropic, except possibly below 90 km.

The apparent anisotropy at Moomba B is partly due to the sparse short-period data. However, the inability of layered model curves to fit the data at long periods shows that the deeper anisotropy at least is significant, probably the results of a lateral conductivity change. These could be either stratigraphic or structural.

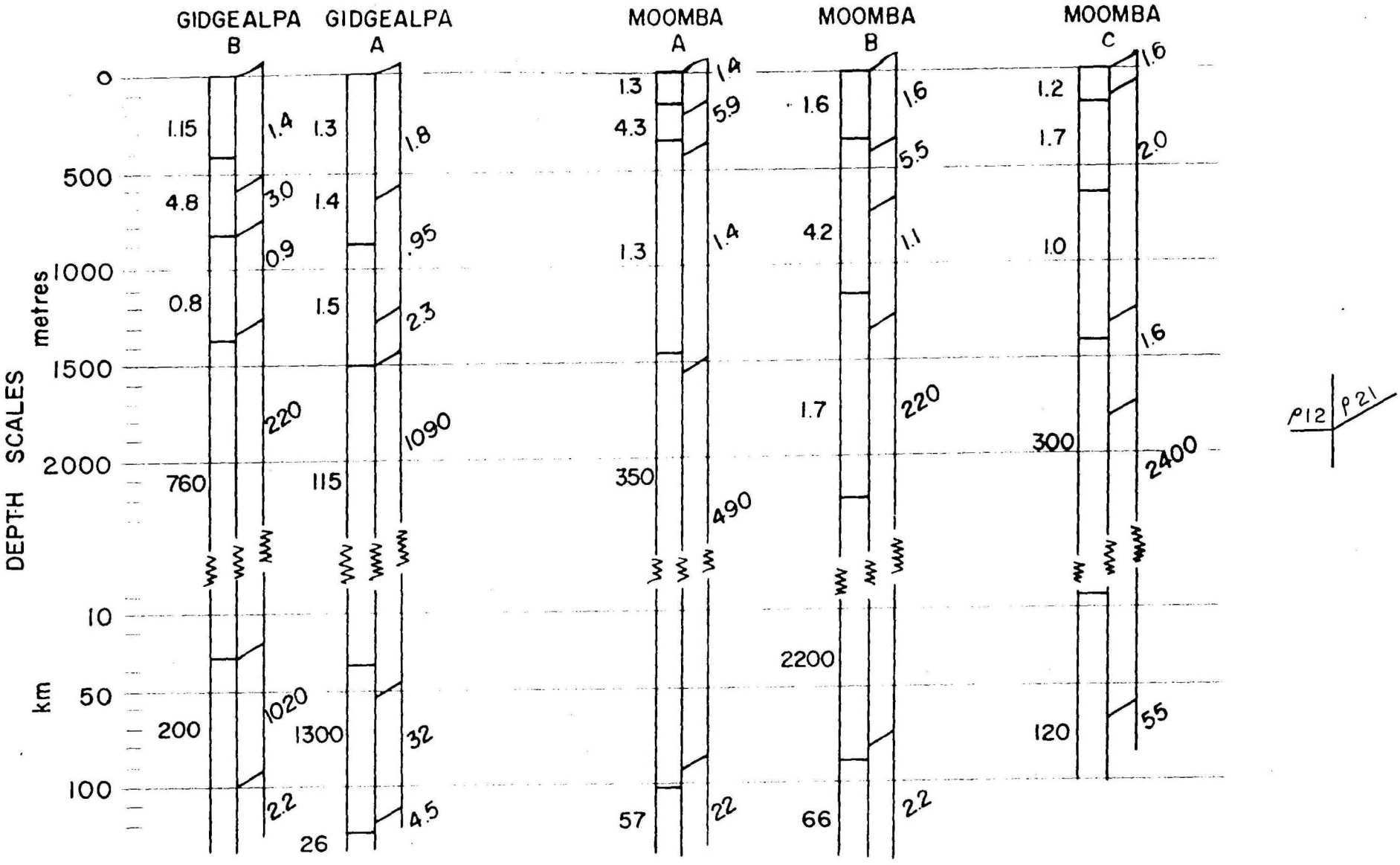

Figure 17 HORIZONTALLY LAYERED INVERSION MODELS FROM ROTATED APPARENT RESISTIVITY AND PHASE CURVES.

Moomba C data do not extend to the longer periods, but the shallow interpretation should be valid. The major difference is in the indicated depths to the resistivity increases in the two data sets. This is very likely to have been caused by the Big Lake Fault separating the Big Lake and Moomba fields, a conclusion which is supported by the Tipper data.

The difference in depths to the rapid rise at Gidgealpa A and B is only marginally significant statistically, but it does accompany a real difference of depth to the Transition Beds of this magnitude as indicated in the structural cross section, Figure 18; this is due to the fact that Gidgealpa B is closer to the axis of the anticline. Good agreement between interpreted (Figure 7) and true depths was obtained for those sites close to the section E-F shown in Figure 18, in particular the depths to the bottom of the Tertiary and the top of the Transition Beds. The Tippers themselves are in terms of ratios, with the arctangent of the (Hz)/(Hxr) ratio shown on the right-hand scale (Hxr is the rotated Hx field). These tipper dip angles which are indicative of layer dips are very similar at periods shorter than 1000 seconds, but Moomba C then continues to increase whereas the others decline. Moomba C is in a different structural area (Big Lake) to the other sites. In the period range where the Tippers are defined best, (i.e. due to the skin depth range being comparable to distance from structure) 100-1000 seconds, the four most westerly sites indicate a strike direction of about 20° which corresponds very well with the direction of the Gidgealpa structure and the major associated faults. The Moomba C direction, 70°, is the same as that of the Big Lake Fault. At shorter periods the inferred strikes at the northern pair of sites (Gidgealpa A and Moomba B) do not change, while at the three southern sites inferred strikes shift to near 140°. At periods longer than 1000 seconds (corresponding to greater distances) Moomba A Tipper responds to the Big Lake Fault or a parallel structure.

One structure which would produce Tipper data such as is observed

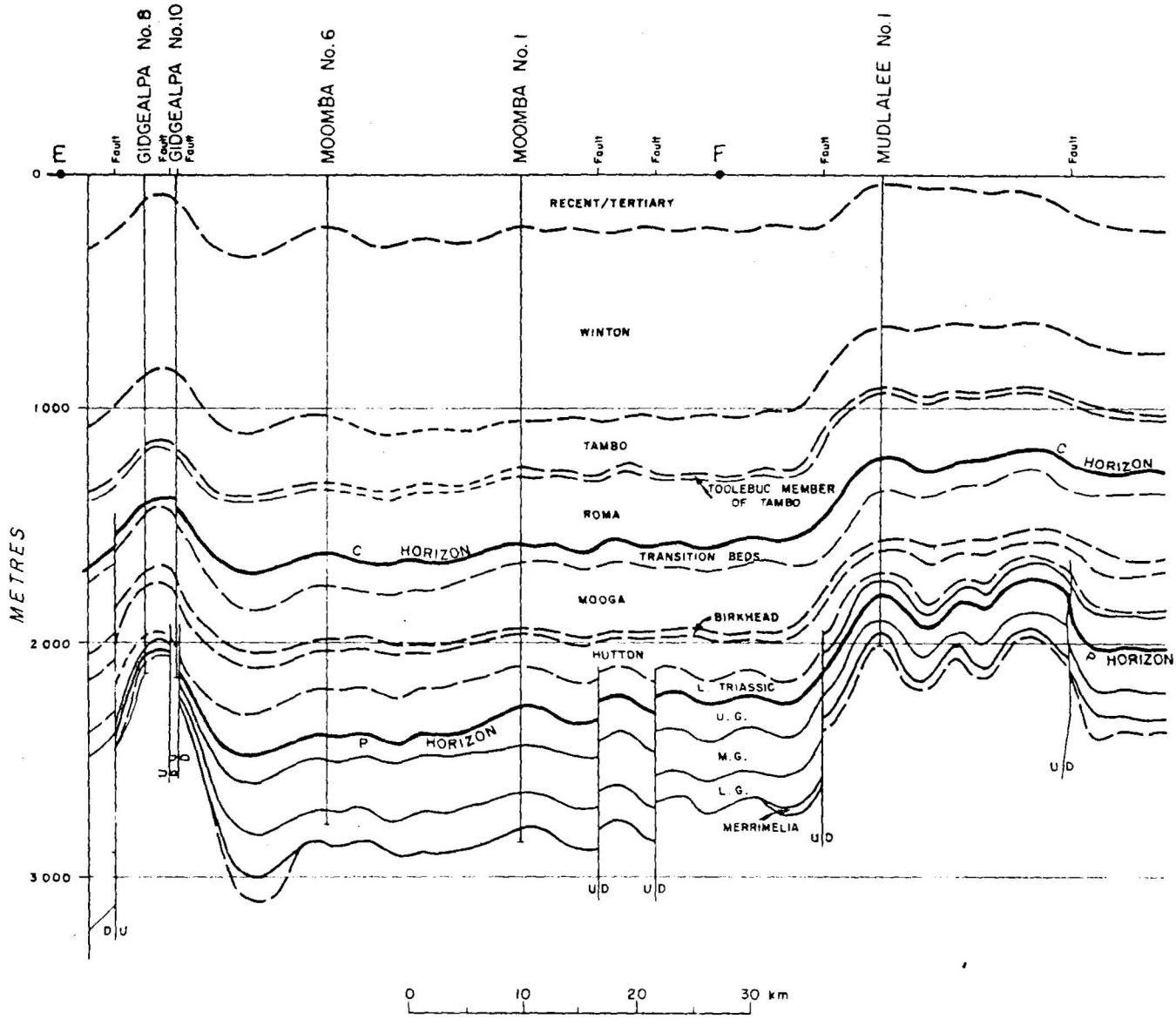

Figure 18 GEOLOGICAL SECTION E—F (see Figure 6)
(constructed from seismic and well data)

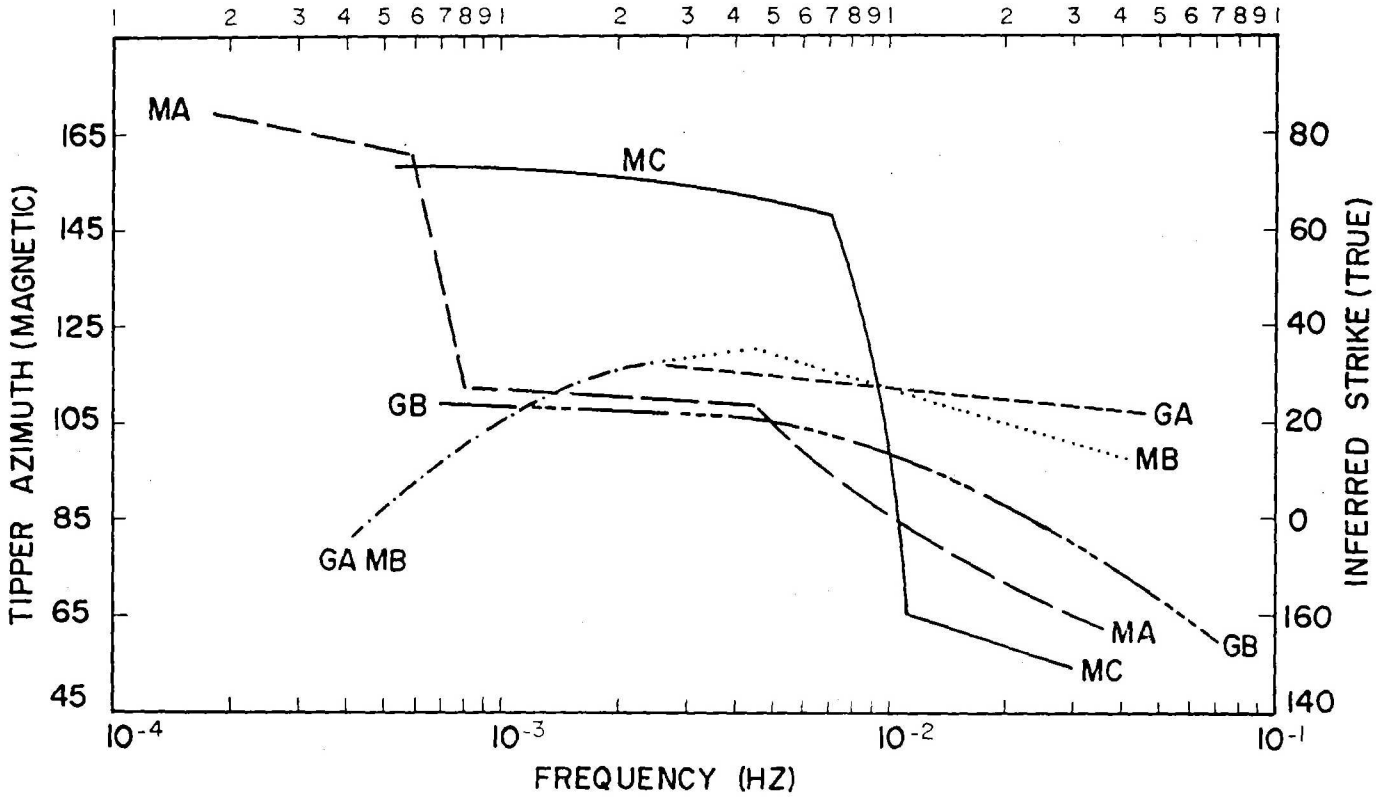

Figure 19 MAGNETIC TIPPER DATA

MA	MOOMBA	A SITE	GA	GIDGEALPA	A SITE
MB	MOOMBA	B SITE	GB	GIDGEALPA	B SITE
MC	MOOMBA	C SITE			

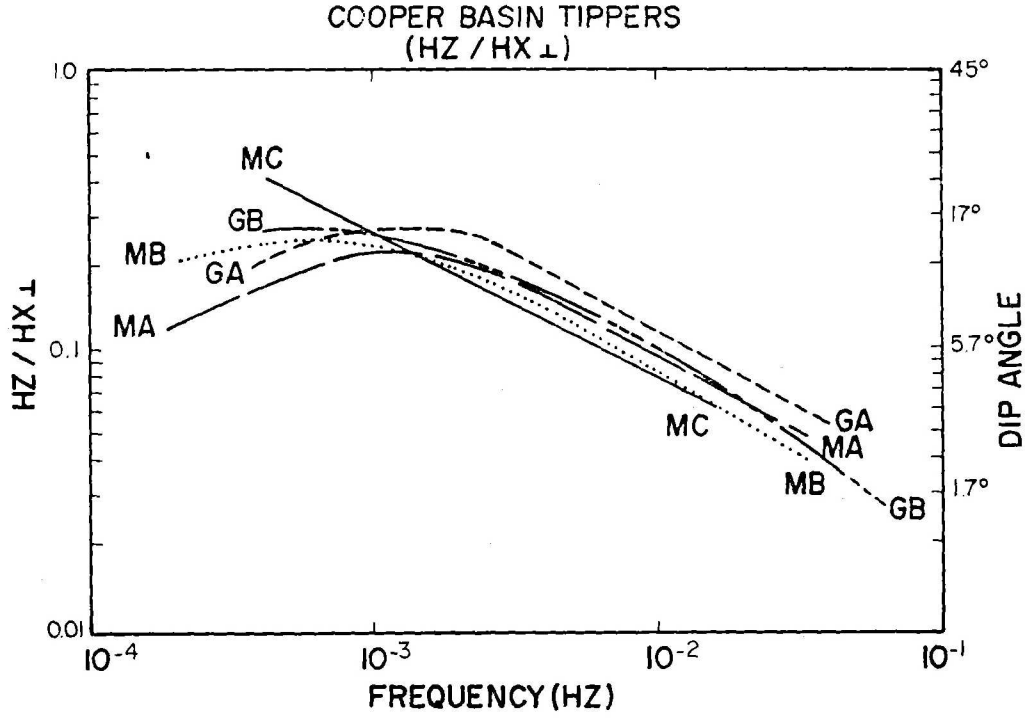

Figure 20 MAGNETIC TIPPER DATA

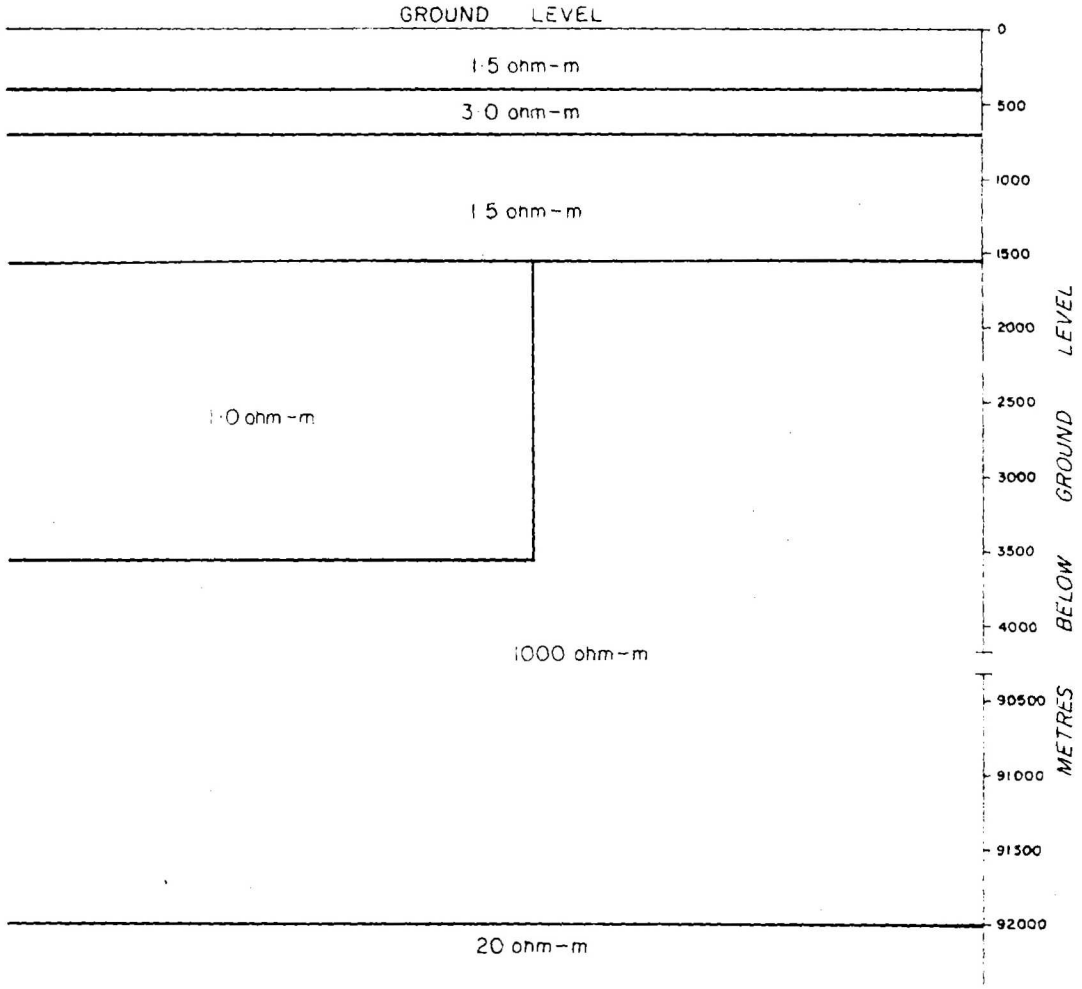

Figure 21 MODEL WHICH WOULD PRODUCE TIPPER DATA
(Figures 19 and 20)

is the 2-dimensional model shown in Figure 21. The conductive block could correspond to the large thickness of Mesozoic material which appears to the west of the Gidgealpa structure, or to the lens of conductive Cenozoic sediments lying along the axis of the Cooper Basin. The contact must in any event have a strike direction near 20°. In this model, all five sites will be on the resistive side of the contact. Site coverage is not extensive enough to permit more positive interpretation. An important observation is that the contact affects the vertical magnetic variation field Hz for several tens of kilometers on the resistive side. The lateral 'vision' of the MT method is considerable.

The tipping vector analysis reports well to the structural situation in the Cooper Basin. As has been mentioned previously the Basin is essentially horizontally layered at the chosen measurement positions. In a horizontally layered medium with the MT assumption of incident plane wave conditions, the inducing magnetic field in the earth is horizontal with zero vertical component. A vertical magnetic field component may be induced by a deflection of telluric currents in the horizontal plane. A perturbation in the telluric current need not be very large to cause a significant increase in vertical magnetic field intensity. The same perturbation would not normally produce a significant effect on the horizontal currents.

9. CONCLUSIONS

The following conclusions can be drawn from this survey:

1. The thickness and conductivity of the younger (Cretaceous) section of the Great Artesian Basin sediments can be mapped by using the Lower Cretaceous Transition Beds as a marker. The top of the water-bearing Mooga Sandstone Formation could also be indirectly mapped as it is overlain by the Transition Beds.

2. The economically important Permian Gidgealpa Group is not mappable either directly from its own electrical properties, or indirectly by mapping those sediments lying above or below the Permo-Triassic section. Significant resistivity contrasts between the older Great Artesian Basin sediments and the Permo-Triassic Section do not exist. The pre-Permian sediments are significantly more resistive than the Permian but are too variable electrically from site to site to be useful as an indirect marker for the base of the Permian.

3. Porosity variations within the Gidgealpa Group were not discernible at these recording sites.

4. No major porous zones below the Permian were apparent at any of the sites recorded on the survey. More widespread measurements might observe deep conductive zones such as those drilled in Kalladeina No. 1. No sites were occupied in the vicinity of this well.

5. The boundary between the pre-Permian section and true basement was not found. This would imply that the resistivity of the pre-Permian sediments must approach the resistivity of the basement.

6. Interesting large-scale features were apparent within the deeper crust. There is a decrease in resistivity observable at four of the sites at a depth of about 90 kilometres. This would most likely be within the upper mantle (see Lilley & Bennett, 1972).

7. This was the second five-component MT survey conducted in Australia by BMR and Macquarie University; the quality of data improved markedly over the first survey as expertise was gained in site preparation and equipment handling, etc. A further improvement has

been experienced on more recent surveys with the collection of more data acquired in far shorter times.

8. The use of Tipper information was made more meaningful with new definitions for Tipper parameters by Jupp and Vozoff (1976) and this led to the detection of faults (i.e. Gidgealpa and Big Lake) located at large lateral distances. The ability of the MT method to locate such structure at considerable lateral distances is of considerable importance for widely spaced reconnaissance work.

9. One of the primary aims of the survey was to test the results obtainable from the MT method against proven data from electric well logs. Figure 22 shows the good agreement between measured MT data and that predicted from nearby well logs.

10. At the three MT sites near the seismic section shown in Figure 18, good agreement is obtained (i.e. $\pm$ 5%) from comparing interpreted depths to the bottom of Tertiary and top of the Transition Beds with the figures obtained by seismic.

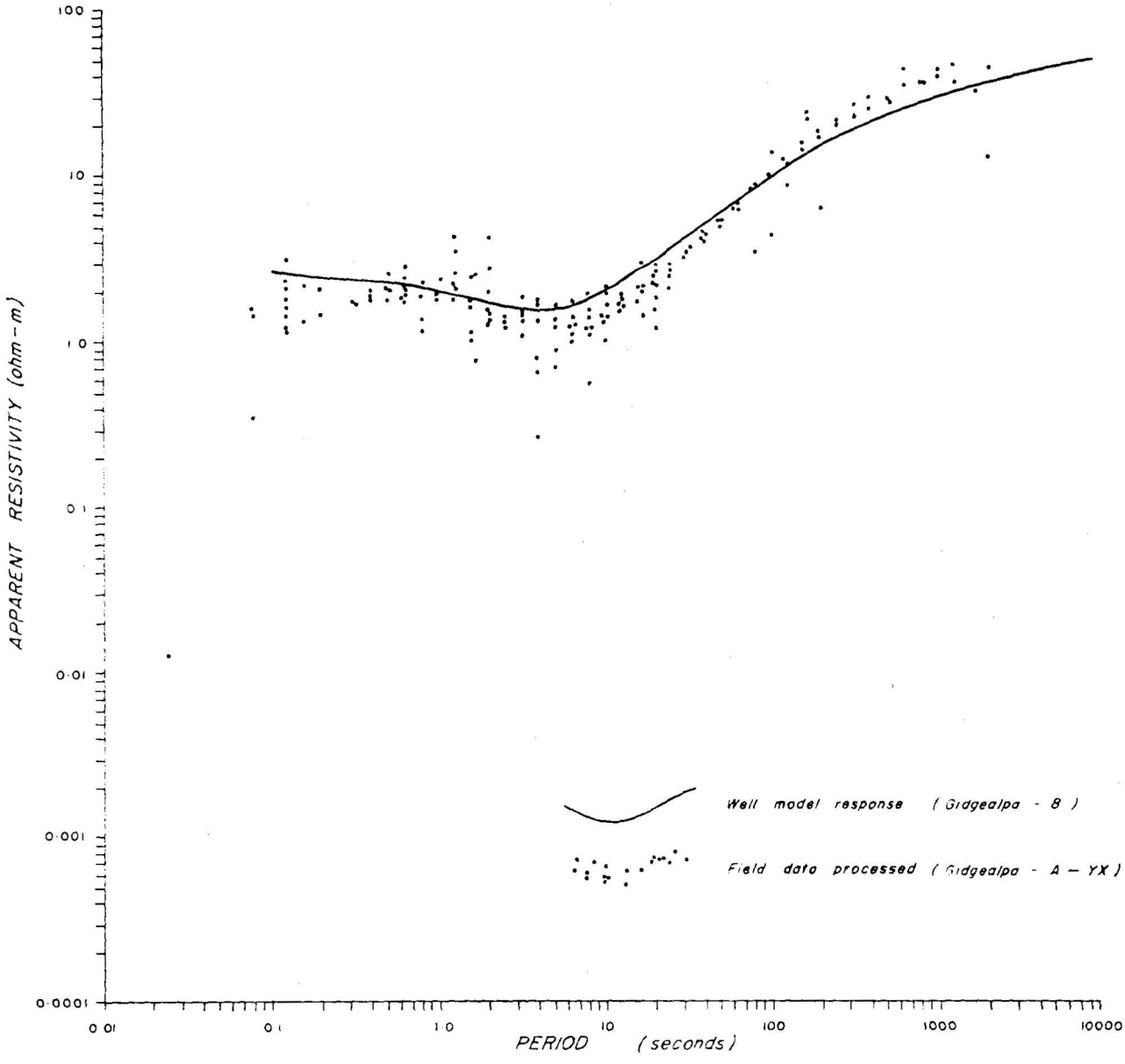

Figure 22 COMPARISON BETWEEN DATA PREDICTED FROM MODELLING AND ACQUIRED IN THE FIELD.

10. REFERENCES

Aero Service Corporation, 1962 - Interpretation of airborne magnetometer surveys in South Australia and Queensland. Internal report (unpublished).

Beddoes, L.R. (Editor), 1972 - Oil and Gas fields of Australia, PNG and NZ 133-88.

Delhi Australian Petroleum Ltd, 1968 - Southwest Cooper Basin gravity survey. Internal report (unpublished).

Delhi Australian Petroleum Ltd, 1969 - Southern Cooper Basin seismic and gravity survey. Internal report (unpublished).

Gatehouse, C.G., 1972 - Formations of the Gidgealpa Group in the Cooper Basin. Australas. Oil Gas Rev., 5, 10-15.

Jupp, D.L.B. and Vozoff, K., 1975 - Stable iterative methods for the inversion of geophysical data. Geophys. J.R. Astr. Soc., 42, 957-76.

Keller, G.C., & Frishknecht, F.C., 1966 - ELECTRICAL METHODS IN GEOPHYSICAL PROSPECTING. Pergamon Press.

Kerr, D.W., Moore, R.F. & Spence, A., in prep. - Field procedures for magnetotelluric surveys. Bur. Miner. Resour. Aust. Rec.

Laherrere, J., & Drayton, R.D., 1965 - Some geophysical results across the Simpson Desert. APEA J., 5, 48-58.

Lilley, F.E.M., & Bennett, D.J., 1972 - An array experiment with magnetic variometers near the coasts of southeast Australia. Geophys. J.R. astr. Soc., 29, 49-64.

Lonsdale, G.F., & Ingall, L.N., 1965 - Strezlecki Creek and Lake Gregory helicopter gravity survey, South Australia (for Delhi Australian Petroleum Ltd). Internal report (unpublished).

Milton, B.E., & Morony, G.K., 1973 - A regional interpretation of the 1:1 000 000 gravity and aeromagnetic maps of the Great Artesian Basin in South Australia. S.A. Dept Mines, R.B. 73/293 (unpublished).

Moore, R.F., 1975 - A magneto-telluric model study of the southern Cooper Basin. M.Sc. Thesis, Macquarie University.

Pollard, P.C., 1971 - Computer programme for producing magneto-telluric curves for a horizontally layered earth, Bur. Miner. Resour. Aust. Rec. 1971/35 (unpublished).

Sims, W.E., & Bostick, F.X., 1969 - Methods of magneto-telluric analysis. Unpublished tech. Rep. 58, Electronics Research Centre, Uni. Texas.

Vozoff, K., 1972 - The magneto-telluric method in the exploration of sedimentary basins. Geophys, 37, 98-141.

Vozoff, K., Kerr, D., Moore, R.F., Jupp, D.L., & Lewis, R.G., 1975 - Murray Basin magneto-telluric study - J. Geol. Soc. Aust., 22, 361-75.

Wopfner, H., 1966 - A case history of the Gidgealpa gas field, South Australia. Australas. Oil Gas J., 12, 29-53.

APPENDIX I

-MTCALC-

A horizontally layered earth MT

modelling program

1. Introduction

MTCALC is a Fortran subroutine written for the CDC 6600 and CDC Cyber 76 computers. It calculates the theoretical magneto-telluric response (apparent resistivity and phase) of a horizontally stratified earth model for vertically incident, plane electromagnetic waves. A model consists of 'n' resistivities, 'n' magnetic permeabilities, 'n' dielectric constants and 'n-1' thicknesses. The theoretical basis of MTCALC follows:

2. Theory

The formula for the impedance of an n-layered earth in response to a vertically incident plane electromagnetic wave is given in MKS units by (Keller & Frischknecht, 1966):

$$Z = \frac{Ex}{Hy} = \frac{Ey}{Hx}$$

$$= \frac{-i\omega\mu}{\gamma_1} \coth\left[\gamma_1 h_1 + \operatorname{arcoth}\left\{\frac{\gamma_1}{\gamma_2}\coth\left(\gamma_2 h_2 + \operatorname{arcoth}\left\{\frac{\gamma_2}{\gamma_3}\left(\gamma_3 h_3 + \operatorname{arcoth}\left\{\frac{\gamma_3}{\gamma_4}\cdots\cdots + \operatorname{arcoth}\left\{\frac{\gamma_{n-3}}{\gamma_{n-2}}\coth\left(\gamma_{n-2} h_{n-2} + \operatorname{arcoth}\left\{\frac{\gamma_{n-2}}{\gamma_{n-1}}\coth\left(\gamma_{n-1} h_{n-1} + \operatorname{arcoth}\frac{\gamma_{n-1}}{\gamma_n}\right)\right\}\right)\right\}\cdots\cdots\right\}\right)\right\}\right)\right\}\cdots\cdots\right\}\right] \quad \text{(1)}$$

where Ex, Ey, Hx and Hy are the electric and magnetic field intensities with respect to an arbitary set of cartesian co-ordinates in the horizontal plane. The symbols ω, γ, μ, h represent the angular velocity of the wave, the propogation constant, the magnetic permeability, and the thickness of each layer, respectively, The subscripts refer to the number of each layer, as shown in Figure 1. The symbol i is the complex number $\sqrt{-1}$. The period of the wave is given by

$$T = \frac{2\pi}{\omega} \text{ in seconds.}$$

The apparent resistivity at a given period is defined by

$$\rho_a = \frac{|Z|^2}{\omega\mu}$$

The phase angle of Z is the difference in phase between the E and the H fields.

3. Subroutine MTCALC

This subroutine calculates apparent resistivity and phase by equation (1) for any number of layers 'n' using

$$A = \coth \Theta = \frac{e^{\Theta} + e^{-\Theta}}{e^{\Theta} - e^{-\Theta}} \quad , \quad \Theta = \operatorname{arcoth} A = \tfrac{1}{2} \log_e \sqrt{\frac{A+1}{A-1}}$$

The routine is a modified version of MAGTEL, a computer program written by Pollard (1971), and a documented listing follows. Input to the calling program is left for the user. Note, however, that both the magnetic permeabilities and dielectric constants need to be multiplied by constants before being passed to MTCALC.

```
      SUBROUTINE MTCALC(N,T0,NT,RHO,H,PE,RHOA,PHA)
C
C       *MTCALC* EVALUATES APPARENT RESISTIVITY AND PHASE FOR
C       AN N-LAYER MODEL FOR DEFINED PERIOD VALUES WHERE EACH
C       LAYER HAS A DISCRETE RESISTIVITY,THICKNESS,MAGNETIC
C       PERMEABILITY AND DIELECTRIC CONSTANT .
C
C       THE FOLLOWING VARIABLES ARE SIGNIFICANT -
C
C    1    N   - THE NUMBER OF LAYERS IN THE MODEL.
C    2    RHO - THE INDIVIDUAL LAYER RESISTIVITIES (N).
C    3    H   - THE INDIVIDUAL LAYER THICKNESSES   (N-1).
C    4    AMU - THE INDIVIDUAL LAYER MAGNETIC PERMEABILITIES EACH
C              MULTIPLIED BY 4.XPIX10.**-7 (N).
C    5    EPS - THE INDIVIDUAL LAYER DIELECTRIC CONSTANTS EACH
C              MULTIPLIED BY 8.854X10**-12 (N).
C    6    NT  - THE NUMBER OF PERIOD VALUES AT WHICH THE APP.RES.,PHASE
C              ARE TO BE EVALUATED.
C    7    T0  - THE INITIAL PERIOD (PERIOD INCREASES BY SQRT(10.))
C    8    PE  - THE PERIOD VALUES USED.
C    9    RHOA- THE APPARENT RESISTIVITIES EVALUATED (NT).
C   10    PHA - THE DIFFERENCES IN PHASE BETWEEN E AND H.
C
C   N.B. GOOD APPROXIMATIONS TO THE MAG. PERM. AND DIEL. CONST. ARE
C              MU=1., EPS=10.
C
      COMPLEX Z,CI,C1,PK(19),ARCOTH,PKH,SUM,COTH,PROD
      DIMENSION RHO(99),H(98),PE(21),RHOA(21),PHA(21)
      COMMON /MOD/ AMU(99),EPS(99)
      CARG(Z)=ATAN2(AIMAG(Z),REAL(Z))
      CI=CMPLX(0.,1.)
      C1=CMPLX(1.,0.)
      PI=3.1415926536
      NMAX=N
      T=T0
      DO 15 J=1,NT
      F=1./T
      IN1=N-1
      IN2=N-2
      DO 77 K=1,N
      BETA=SQRT(1.+1./(4.*PI*PI*F*F*RHO(K)**2*EPS(K)**2))-1.
      BETA=2.*PI*F*SQRT(.5*AMU(K)*EPS(K)*BETA)
      ALPHA=SQRT(BETA*BETA+4.*PI*PI*F*F*AMU(K)*EPS(K))
   77 PK(K)=CMPLX(ALPHA,BETA)
      ARCOTH=CLOG(CSQRT((PK(IN1)/PK(N)+C1)/(PK(IN1)/PK(N)-C1)))
      DO 6 I=1,NMAX
      IF(I.EQ.1) GO TO 8
      ARCOTH=CLOG(CSQRT((PROD+C1)/(PROD-C1)))
    8 PKH=PK(IN1)*H(IN1)
      SUM=ARCOTH+PKH
      COTH=(CEXP(SUM)+CEXP(-SUM))/(CEXP(SUM)-CEXP(-SUM))
      IF(N.EQ.2) GO TO 9
      PROD=PK(IN2)/PK(IN1)*COTH
      N=N-1
      IN1=IN1-1
    6 IN2=IN2-1
    9 Z=CI*8.*PI*PI*F*10.**(-7)/PK(1)*COTH
      N=NMAX
      PE(J)=T
      RHOA(J)=CABS(CI*Z*Z/(8.*PI*PI*F*10.**(-7)))
      PHA(J)=CARG(Z)*180./PI
   15 T=T*SQRT(10.)
      RETURN
      END
```

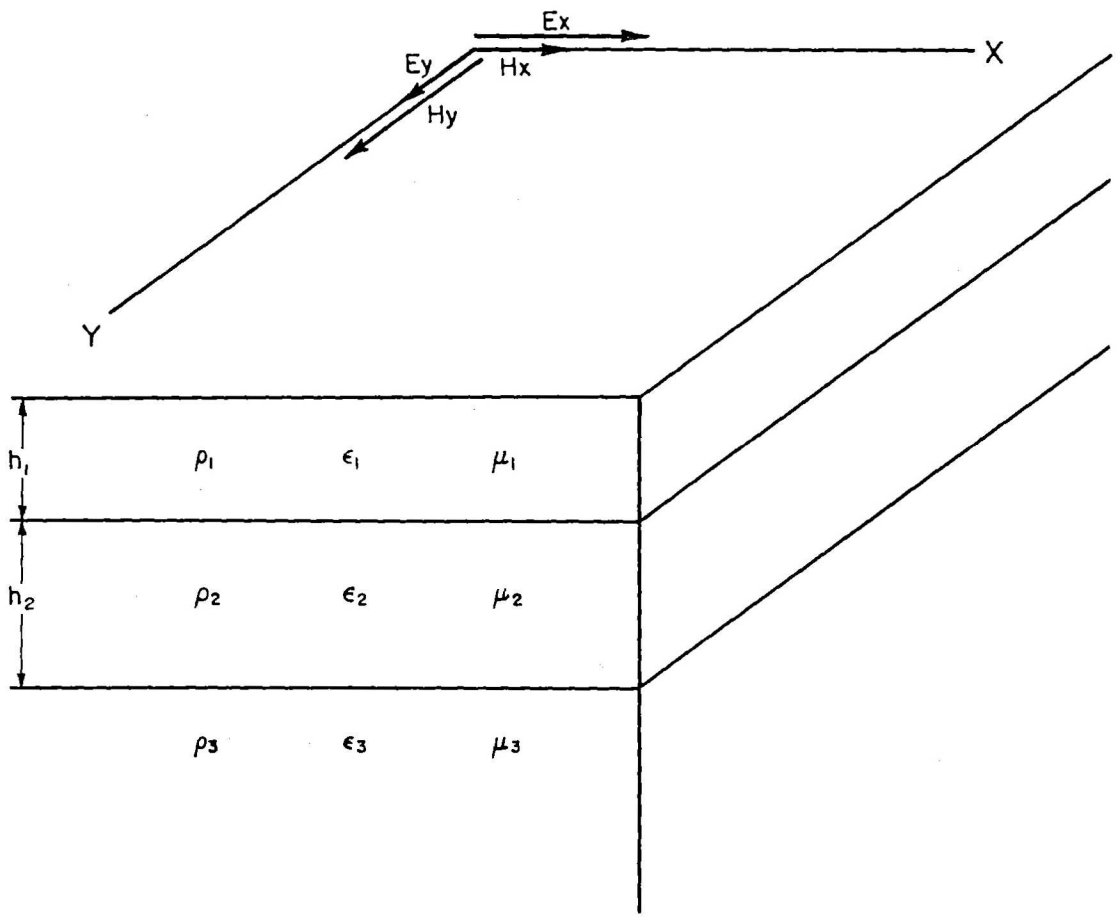

SKETCH OF A PLANE WAVE INCIDENT
ON A 3-LAYER EARTH

Figure A

- Macquarie University

Academic Staff	Professor K. Vozoff
	Dr R. Lewis
Technical Officers	K. Gibbons
	R. Nurse
Student	M. Asten

3. Equipment

MT analogue	BMR	Macquarie University
E-field preamplifiers	Geotronics MTE-4	
E-field sensors		$Cd/CdCl_2$ porous pots
H-field preamplifiers	Geotronics MTH-4	
H-field sensors	Geotronics MTC-4SS	
Filter/postamplifiers	Geotronics MTF-15	
Calibrator	Geotronics MTC-2	

Computer acquisition system

Computer	H.P. 2116B	Interdata Model 10
Magnetic tape drive	H.P. 7970A	Interdata (9 track)
Keyboard/printer	NCR 260	ASR 35
Paper tape reader	H.P. 2748A	
Paper tape punch	H.P. 2753A	
A/D converter	Raytheon Multiverter (custom-built)	

Auxiliary equipment

CRO	Techtronix 4 channel storage	H.P. 2 channel
DVM	H.P. 3440A	
Function generator	H.P. 3300A	
Chart recorder		YEW-UV recorder

APPENDIX 2

Operational data, staff and equipment

1. Operational Data

Sedimentary basin	Cooper Basin in South Australia
Survey area	Innamincka 1:250 000 Sheet
Survey dates -	
7 Aug - 10 Aug	Equipment installation in Macquarie University trailer (in Sydney)
14 Aug	Depart Canberra (for Sydney)
17 Aug	Depart Sydney (for Moomba)
24 Aug	Arrive Moomba
24 Aug - 26 Aug	Equipment testing and repairs
25 Aug.	D. Kerr, K. Vozoff arrive (by air)
27 Aug - 30 Aug	Recording at site 1: Moomba A
31 Aug - 3 Sept	Recording at site 2: Moomba B
4 Sept - 6 Sept	Recording at site 3: Gidgealpa A
4 Sept	K. Vozoff departs for Sydney
5 Sept	D. Kerr departs for Canberra
7 Sept - 9 Sept	Recording at site 4: Gidgealpa B
10 Sept - 12 Sept	Recording at site 5: Moomba C
13 Sept	Depart (for Sydney)
20 Sept	Arrive Sydney
24 Sept	Return to Canberra
Number of sites	5
Number of files recorded	166

2. Staff

- BMR

Supervisor	M.G. Allen (Geophysical Services Section)
Party Leader	R.F. Moore
Geophysicist	D.W. Kerr
Mechanic	S. D'Arcy

Vehicles	BMR	Macquarie University
Instrument van		Converted radar trailer
Trucks - 3 ton		IH 4 x 4 (ex Army)
- 30 cwt	D1310 (4 x 4)	
Land Rover	LWB	
Generator	Ford/Dunlite	
	Lister/Proline alternators	

APPENDIX 3

An Example of the Information output from the MT processing software for a single data file

```
GIDGEALPA B - 1700/8/9/744 - DC-.025 ********** 4096/10000
GIDGEALPA B - 1700/8/9/744 - DC-.025 ********** 4096/10000
GIDGEALPA B - 1700/8/9/744 - DC-.025 ********** 4096/10000
GIDGEALPA B - 1700/8/9/744 - DC-.025 ********** 4096/10000
GIDGEALPA B - 1700/8/9/744 - DC-.025 ********** 4096/10000
```

CHANNEL ORDER = 1,2,3,4,5

FREQUENCY INCREMENT = .488281E-04 HERTZ.
WIRE LENGTHS IN METRES:-
EX= 1000 METRES
EY= 1000 METRES

AVERAGED AUTO POWER SPECTRA

FREQUENCY	EX	EY	HZ	HX	HY
.1941E-03	.131E+02	.134E+01	.149E+08	.932E+08	.139E+09
.2426E-03	.736E+01	.102E+01	.145E+07	.240E+08	.108E+09
.2911E-03	.450E+01	.104E+01	.124E+07	.800E+07	.776E+08
.3881E-03	.100E+01	.327E+00	.477E+06	.484E+07	.325E+07
.4852E-03	.148E+00	.125E+00	.427E+05	.895E+06	.102E+07
.5822E-03	.431E-01	.588E-01	.270E+05	.450E+06	.263E+06
.7762E-03	.224E-01	.393E-01	.139E+05	.270E+06	.959E+05
.9703E-03	.134E-01	.459E-02	.428E+04	.308E+05	.710E+05
.1213E-02	.238E-02	.882E-03	.319E+03	.353E+04	.812E+04
.1552E-02	.836E-03	.602E-03	.143E+03	.224E+04	.272E+04
.1941E-02	.829E-03	.254E-03	.993E+02	.699E+03	.217E+04
.2474E-02	.278E-03	.103E-03	.389E+02	.278E+03	.700E+03
.3105E-02	.902E-04	.412E-04	.876E+01	.856E+02	.215E+03
.3930E-02	.102E-04	.169E-04	.830E+00	.368E+02	.288E+02
.4948E-02	.467E-05	.936E-05	.205E+00	.188E+02	.131E+02
.6259E-02	.222E-05	.284E-05	.824E-01	.551E+01	.560E+01
.7903E-02	.217E-05	.178E-05	.642E-01	.344E+01	.420E+01
.9934E-02	.149E-05	.105E-05	.304E-01	.198E+01	.345E+01
.1261E-01	.145E-05	.119E-05	.258E-01	.214E+01	.309E+01
.1591E-01	.744E-06	.408E-06	.867E-02	.714E+00	.158E+01
.2004E-01	.210E-06	.180E-06	.189E-02	.277E+00	.417E+00
.2523E-01	.739E-07	.541E-07	.503E-03	.943E-01	.133E+00
.3192E-01	.265E-07	.181E-07	.110E-03	.304E-01	.554E-01
.4022E-01	.530E-08	.358E-08	.227E-04	.540E-02	.189E-01

AMPLITUDE COHERENCIES

FREQUENCY	EXEY	EXHZ	EXHX	EXHY	EYHZ	EYHX	EYHY	HXHZ	HYHZ	HXHY
.1941E-03	.97	.90	.79	.74	.57	.67	.81	.58	.80	.34
.2426E-03	.91	.96	.60	.93	.92	.64	.84	.54	.96	.34
.2911E-03	.78	.96	.38	.97	.85	.79	.75	.26	.92	.21
.3881E-03	.60	.97	.72	.97	.63	.97	.50	.75	.90	.60
.4852E-03	.68	.72	.62	.92	.61	.96	.59	.67	.54	.43
.5822E-03	.73	.83	.68	.79	.64	.94	.54	.71	.62	.29
.7762E-03	.82	.94	.80	.95	.91	.99	.74	.91	.86	.69
.9703E-03	.85	.92	.83	.98	.86	.98	.91	.90	.91	.89
.1213E-02	.47	.97	.47	.91	.46	.96	.27	.51	.88	.28
.1552E-02	.37	.89	.29	.96	.35	.97	.42	.22	.83	.37
.1941E-02	.68	.97	.63	.98	.62	.98	.72	.57	.97	.68
.2474E-02	.18	.97	.09	.96	.29	.99	.20	.23	.89	.18
.3105E-02	.46	.98	.37	.93	.49	.99	.38	.40	.87	.32
.3830E-02	.05	.90	.05	.83	.42	1.00	.04	.42	.78	.07
.4949E-02	.38	.82	.36	.92	.30	1.00	.33	.28	.78	.32
.6258E-02	.00	.88	.03	.85	.45	1.00	.14	.46	.70	.14
.7908E-02	.21	.91	.25	.97	.54	1.00	.17	.57	.86	.22
.9994E-02	.21	.91	.26	.98	.53	1.00	.24	.60	.91	.27
.1261E-01	.54	.92	.53	.99	.78	1.00	.53	.78	.90	.52
.1591E-01	.70	.94	.69	.98	.83	1.00	.71	.83	.95	.70
.2004E-01	.73	.93	.72	.95	.85	1.00	.74	.86	.93	.73
.2528E-01	.88	.96	.88	.98	.94	1.00	.86	.94	.94	.86
.3193E-01	.85	.93	.84	.92	.90	1.00	.77	.91	.85	.76
.4022E-01	.81	.83	.84	.71	.73	.92	.60	.80	.58	.62

CAGNIARD RESISTIVITIES

FREQUENCY	PERIOD	RESXY	PHZXY	COHXY	
.194E-03	.515E+04	97.05	11.10	.74	
.243E-03	.412E+04	56.01	43.49	.93	**
.291E-03	.344E+04	39.87	38.02	.97	**
.388E-03	.258E+04	158.65	36.53	.97	**
.485E-03	.206E+04	59.82	23.37	.92	**
.582E-03	.172E+04	56.36	43.14	.79	
.776E-03	.129E+04	60.26	37.53	.95	**
.970E-03	.103E+04	39.04	31.54	.98	**
.121E-02	.824E+03	47.94	28.80	.91	**
.155E-02	.644E+03	38.58	18.61	.96	**
.194E-02	.515E+03	38.31	17.13	.98	**
.247E-02	.404E+03	32.10	23.60	.96	**
.310E-02	.322E+03	27.03	21.42	.93	**
.393E-02	.254E+03	17.97	4.44	.83	**
.495E-02	.202E+03	14.44	12.39	.92	**
.626E-02	.160E+03	12.66	12.27	.85	**
.791E-02	.126E+03	13.05	10.81	.97	**
.999E-02	.100E+03	8.64	8.79	.98	**
.126E-01	.793E+02	7.42	10.51	.99	**
.159E-01	.628E+02	5.93	13.49	.99	**
.200E-01	.493E+02	5.04	16.79	.99	**
.253E-01	.396E+02	4.40	21.46	.98	**
.319E-01	.313E+02	2.99	29.46	.92	**
.402E-01	.249E+02	1.40	41.30	.71	

CAGNIARD RESISTIVITIES

FREQUENCY	PERIOD	RESYX	PHZYX	COHYX	
.194E-03	.515E+04	14.81	238.55	.67	
.243E-03	.412E+04	34.95	197.97	.64	
.291E-03	.344E+04	88.99	229.24	.79	
.388E-03	.258E+04	34.90	222.23	.97	**
.435E-03	.206E+04	57.58	229.65	.96	**
.582E-03	.172E+04	44.74	227.31	.94	**
.776E-03	.129E+04	37.35	214.04	.99	**
.970E-03	.103E+04	30.69	208.38	.98	**
.121E-02	.824E+03	41.14	224.31	.96	**
.155E-02	.644E+03	34.63	208.63	.97	**
.194E-02	.515E+03	37.52	210.82	.99	**
.247E-02	.404E+03	30.03	202.60	.99	**
.310E-02	.322E+03	31.00	199.21	.99	**
.388E-02	.254E+03	23.42	196.48	1.00	**
.495E-02	.202E+03	19.93	195.10	1.00	**
.626E-02	.160E+03	16.49	192.40	1.00	**
.791E-02	.126E+03	13.17	190.88	1.00	**
.999E-02	.100E+03	10.61	189.49	1.00	**
.126E-01	.793E+02	8.81	187.82	1.00	**
.159E-01	.628E+02	7.18	186.72	1.00	**
.200E-01	.499E+02	5.76	187.16	1.00	**
.253E-01	.396E+02	4.54	187.31	1.00	**
.318E-01	.313E+02	3.73	189.20	1.00	**
.402E-01	.249E+02	3.30	191.99	.92	**

TIPPING VECTOR ANALYSIS

FREQUENCY	PERIOD	TIPPER	TIP-PHZ	ANG2D	ANG3D	T-SKEW	PCOH-HZ
.194E-03	.515E+04	.30	43.62	124.61	212.49	811E-01	.91
.243E-03	.412E+04	.12	80.24	196.86	239.03	.230E+00	.99
.291E-03	.344E+04	.14	58.42	184.73	243.63	.882E+00	.94
.388E-03	.258E+04	.31	38.60	250.06	246.73	.145E+00	.95
.485E-03	.206E+04	.14	51.87	189.27	206.39	.451E+00	.73
.582E-03	.172E+04	.26	50.21	168.87	218.75	.979E+00	.92
.776E-03	.129E+04	.23	20.37	231.82	232.70	.824E-01	.97
.970E-03	.103E+04	.32	7.94	213.86	211.97	.270E+00	.96
.121E-02	.824E+03	.19	31.59	268.27	195.50	.889E+00	.94
.155E-02	.644E+03	.25	2.83	242.34	242.00	.670E-01	.93
.194E-02	.515E+03	.25	23.77	248.89	221.33	.132E+00	.98
.247E-02	.404E+03	.26	18.03	235.56	220.40	.217E+00	.97
.310E-02	.322E+03	.22	18.96	234.21	219.67	.413E+00	.94
.388E-02	.254E+03	.15	49.80	223.61	144.84	.585E+00	.89
.495E-02	.202E+03	.13	46.03	234.63	155.99	.472E+00	.91
.626E-02	.160E+03	.12	45.35	218.61	144.37	.549E+00	.89
.791E-02	.126E+03	.12	50.14	220.02	132.75	.520E+00	.98
.988E-02	.100E+03	.09	53.94	221.11	121.15	.433E+00	.98
.126E-01	.793E+02	.02	49.99	211.20	125.53	.550E+00	.93
.159E-01	.628E+02	.07	51.09	210.28	122.74	.567E+00	.99
.200E-01	.499E+02	.06	51.94	208.46	118.79	.562E+00	.99
.253E-01	.396E+02	.06	42.25	200.97	137.35	.630E+00	.99
.319E-01	.313E+02	.05	28.93	194.09	161.99	.575E+00	.96
.402E-01	.249E+02	.05	11.25	185.09	179.53	.213E+00	.81

ROTATED TENSOR ANALYSIS

FREQUENCY FREQUENCY	PERIOD PERIOD	RES-XX PHZ-XX	RES-XY PHZ-XY	RES-YX PHZ-YX	RES-YY PHZ-YY	THETA SKEW	PCOH-EX PCOH-EY	
.194E-03	.515E+04	13.48	98.74	2.98	9.84	-34.84	.96	**
.194E-03	.515E+04	77.38	38.66	81.10	54.82	764E+00	.66	
.243E-03	.412E+04	6.32	77.53	.51	5.14	-32.77	.65	
.243E-03	.412E+04	77.93	41.09	142.46	66.00	.530E+00	.83	**
.291E-03	.344E+04	1.79	74.28	19.49	2.25	-41.59	1.00	**
.291E-03	.344E+04	26.38	32.69	257.19	328.27	.204E+00	.98	**
.388E-03	.258E+04	1.55	117.69	35.87	2.39	-13.44	.99	**
.388E-03	.258E+04	31.04	31.22	228.50	53.66	.184E+00	.91	**
.485E-03	.206E+04	3.37	21.23	64.38	1.24	31.47	.93	**
.485E-03	.206E+04	343.37	24.07	222.61	139.64	.747E-01	.97	**
.582E-03	.172E+04	.05	9.75	64.39	.12	41.67	.74	
.582E-03	.172E+04	60.76	73.71	220.11	83.77	.519E-01	.99	**
.776E-03	.129E+04	.69	53.42	21.20	.93	-44.87	1.00	**
.776E-03	.129E+04	121.06	33.35	138.82	346.26	.593E-01	.93	**
.970E-03	.103E+04	2.75	51.35	27.36	3.69	-23.96	.93	**
.970E-03	.103E+04	115.03	32.67	184.37	29.43	.219E+00	.99	**
.121E-02	.824E+03	.97	29.73	49.49	.87	-32.64	.88	**
.121E-02	.824E+03	258.93	17.61	228.07	280.73	.156E+00	.93	**
.155E-02	.644E+03	.27	42.57	29.20	.25	-29.57	.98	**
.155E-02	.644E+03	88.12	17.74	207.43	88.93	.864E-01	.96	**
.194E-02	.515E+03	.61	42.12	34.30	.69	-21.09	.99	**
.194E-02	.515E+03	291.01	8.74	213.40	327.81	.127E+00	.97	**
.247E-02	.404E+03	.92	41.41	21.48	1.04	-40.33	.98	**
.247E-02	.404E+03	44.59	24.88	200.81	57.03	.178E+00	.96	**
.310E-02	.322E+03	.99	32.10	20.75	1.49	-44.51	.95	**
.310E-02	.322E+03	52.76	26.54	195.09	100.56	.199E+00	.98	**
.393E-02	.254E+03	.05	12.57	23.32	.03	-.33	.86	**
.393E-02	.254E+03	90.92	4.24	196.46	59.90	.463E-01	.98	**
.495E-02	.202E+03	.01	11.41	19.87	.02	-9.75	.91	**
.495E-02	.202E+03	268.97	10.81	195.11	140.67	.155E-01	.99	**

.626E-02	.160E+03	.10	9.39	16.62	.06	8.81	.91	**
.626E-02	.160E+03	59.37	11.56	192.52	33.50	.754E-01	.95	**
.791E-02	.126E+03	.12	12.72	12.93	.02	-22.50	.99	**
.791E-02	.126E+03	42.04	10.42	190.37	54.00	.661E-01	.99	**
.999E-02	.100E+03	.10	8.49	10.58	.00	-22.50	.99	**
.999E-02	.100E+03	316.54	7.42	192.43	178.78	.467E-01	.99	**
.126E-01	.793E+02	.03	7.13	8.68	.02	5.12	1.00	**
.126E-01	.793E+02	33.48	12.08	189.24	22.66	.540E-01	.99	**
.159E-01	.628E+02	.01	5.72	7.23	.00	-22.50	.99	**
.159E-01	.628E+02	272.11	11.00	189.30	105.45	.788E-02	1.00	**
.200E-01	.499E+02	.00	4.78	5.68	.01	-7.17	.99	**
.200E-01	.499E+02	237.17	15.93	189.16	44.00	.923E-02	.99	**
.253E-01	.396E+02	.09	3.38	4.30	.03	-14.23	1.00	**
.253E-01	.396E+02	68.20	27.84	187.54	104.61	.117E+00	.98	**
.319E-01	.313E+02	.41	1.73	3.43	.16	-19.37	.93	**
.319E-01	.313E+02	87.34	49.68	184.28	136.76	.322E+00	.98	**
.402E-01	.249E+02	1.30	.85	2.46	.45	-24.12	.72	
.402E-01	.249E+02	80.04	81.89	176.05	153.02	.834E+00	.66	

XXXUNROTATED TENSOR ANALYSISXXX

FREQUENCY FREQUENCY	PERIOD PERIOD	RES-XX PHZ-XX	RES-XY PHZ-XY	RES-YX PHZ-YX	RES-YY PHZ-YY	PCOH-EX PCOH-EY	PREDICTABILITY TENSOR SKEW	
.194E-03	.515E+04	72.39	41.35	5.38	5.88	1.00	.886E+00	**
.194E-03	.515E+04	54.89	25.29	215.78	190.61	.99	.764E+00	**
.243E-03	.412E+04	38.38	38.74	7.13	4.24	1.00	.887E+00	**
.243E-03	.412E+04	56.63	36.93	215.81	190.34	.94	.530E+00	**
.291E-03	.344E+04	18.92	35.05	40.20	3.64	.99	.956E+00	**
.291E-03	.344E+04	2.09	40.12	234.24	190.67	1.00	.204E+00	**
.388E-03	.258E+04	5.88	112.76	37.96	.91	.99	.645E+00	**
.388E-03	.258E+04	23.43	32.41	223.96	104.57	.98	.164E+00	**
.485E-03	.206E+04	5.21	39.25	43.52	2.24	.96	.811E+00	**
.485E-03	.206E+04	37.72	21.46	229.53	233.36	.98	.747E-01	**
.582E-03	.172E+04	9.02	25.49	32.68	7.12	.94	.919E+00	**
.582E-03	.172E+04	26.48	50.16	228.63	197.44	.98	.519E-01	**
.776E-03	.129E+04	3.55	40.26	31.01	1.43	.99	.521E+00	**
.776E-03	.129E+04	53.35	21.12	215.30	238.97	.99	.593E-01	**
.970E-03	.103E+04	8.26	54.63	21.56	.70	.99	.204E+00	**
.970E-03	.103E+04	85.13	21.94	198.92	330.14	.98	.219E+00	**
.121E-02	.824E+03	6.67	34.59	39.28	.51	.94	.924E+00	**
.121E-02	.824E+03	273.15	27.49	221.69	102.70	.98	.156E+00	**
.155E-02	.644E+03	.48	38.82	32.12	.88	.96	.860E+00	**
.155E-02	.644E+03	25.93	19.70	204.79	129.58	.99	.864E-01	**
.194E-02	.515E+03	2.81	42.32	32.50	.09	.99	.532E+00	**
.194E-02	.515E+03	300.40	12.18	209.85	63.18	.99	.127E+00	**
.247E-02	.404E+03	3.51	32.00	29.27	.08	.99	.966E+00	**
.247E-02	.404E+03	42.86	24.58	201.71	117.54	.99	.178E+00	**
.310E-02	.322E+03	3.05	23.03	29.11	.13	.95	.896E+00	**
.310E-02	.322E+03	72.32	25.63	197.72	115.29	.99	.199E+00	**
.393E-02	.254E+03	.05	12.58	23.32	.03	.84	.995E+00	**
.393E-02	.254E+03	92.56	4.23	196.47	59.16	1.00	.463E-01	**
.495E-02	.202E+03	.07	11.54	19.68	.03	.92	.898E+00	**
.495E-02	.202E+03	229.75	11.63	194.50	74.15	1.00	.155E-01	**

.626E-02	.160E+03	.19	9.52	16.43	.01	.86	.981E+00	**
.626E-02	.160E+03	44.89	12.00	192.19	62.22	1.00	.754E-01	**
.791E-02	.126E+03	.09	12.24	13.42	.03	.98	.951E+00	**
.791E-02	.126E+03	43.98	9.87	190.90	47.61	1.00	.661E-01	**
.999E-02	.100E+03	.10	8.29	10.76	.02	.98	.929E+00	**
.999E-02	.100E+03	286.58	10.03	190.10	40.01	1.00	.467E-01	**
.126E-01	.793E+02	.03	7.16	8.66	.01	.99	.728E+00	**
.126E-01	.793E+02	26.95	13.10	189.19	31.10	1.00	.540E-01	**
.159E-01	.628E+02	.02	5.95	6.99	.01	.99	.511E+00	**
.159E-01	.628E+02	215.78	12.12	188.85	22.31	1.00	.788E-02	**
.200E-01	.499E+02	.00	4.85	5.61	.01	.99	.469E+00	**
.200E-01	.499E+02	186.87	16.03	189.02	17.54	1.00	.923E-02	**
.253E-01	.396E+02	.17	3.24	4.38	.01	.98	.263E+00	**
.253E-01	.396E+02	89.99	26.24	189.20	25.86	1.00	.117E+00	**
.319E-01	.313E+02	.85	1.37	3.50	.01	.95	.421E+00	**
.319E-01	.313E+02	110.07	42.64	190.73	34.99	1.00	.322E+00	**
.402E-01	.249E+02	2.32	.21	2.53	.01	.90	.621E+00	**
.402E-01	.249E+02	114.68	71.07	193.62	59.49	.92	.834E+00	**

1:250,000

PLATE I

SURVEY
DELHI AUSTRALIAN PETROLEUM LTD.
IN
UNITED GEOPHYSICAL CORPORATION
SOUTHERN COOPER BASIN
SEISMIC SURVEY
SOUTH AUSTRALIA

BOUGUER GRAVITY

CONTOUR INTERVAL 5 MGAL
DATUM LEVEL SEA LEVEL DATE JULY, 1971

LEGEND

- SEISMIC SHOT POINT (UNITED)
- SHOT POINTS
- REFRACTION SHOT POINT
- PERMANENT MARKER
- ASTRO FIX
- TELLURIOMETER STATION

MAP DATA

CONTROL: HORIZONTAL - BASIC FIRST ORDER CONTROL PROVIDED BY DELHI AUSTRALIAN DEPT. OF LANDS (TELLUROMETER SURVEY, 1966)
SECOND ORDER CONTROL PROVIDED BY DELHI AUSTRALIAN PETROLEUM LTD AND DEPT. OF NATIONAL MAPPING ASTRONOMIC
THIRD ORDER CONTROL PROVIDED BY SEISMIC LOOP CLOSURE ACCURACY VARIES AT 0.5 LENGTH OF TRAVERSE (IN MILES)
VERTICAL - S.A. DEPT. OF LANDS, LYNDHURST-INNAMINCKA LEVEL TRAVERSE, THIRD ORDER CONTROL PROVIDED BY SEISMIC LOOP TRAVERSE, ACCURACY ± 0.5 VIT (IN LENGTH OF TRAVERSE IN MILES)

EXPLANATION

RELATIVE BOUGUER ANOMALIES ARE BASED ON THE VALUES OF THE FOLLOWING 1962 B.M.R. HELICOPTER BASE STATIONS BR10, BR28, DD17, DD31, DD56, T1, T28, T30 AND THE VALUE OF THE INNAMINCKA ISOGAL STATION, ADJUSTED TO TIE GUILPIE P.S. (VALUE USED 979 114·58 mg). LATITUDE CORR. BASED ON 1930 INTERNATIONAL GRAVITY FORMULA. PROBABLE ACCURACY OF GRAVITY VALUES AT SEISMIC SHOT POINTS ±0·10mgl PROBABLE ACCURACY OF HELICOPTER VALUES ±1·50mgl

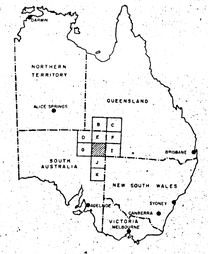

TRANSVERSE MERCATOR PROJECTION
Figures from R.A.S.C. tables based on CLARKE'S 1858 SPHEROID
Compiled by J.R.Homer, senior draftsman Delhi Australian Petroleum Ltd.

SCALE 1:250,000

SOUTH AUSTRALIA
QUEENSLAND
N.S.W.
QLD.
N.S.W.

Record No 1977/41

H54/B13-6

SHEET "H"

1:250,000

PLATE 2

DELHI AUSTRALIAN PETROLEUM LTD.
for
UNITED GEOPHYSICAL CORPORATION

SOUTHERN COOPER BASIN SEISMIC SURVEY
SOUTH AUSTRALIA

"C" HORIZON
(TOP OF TRANSITION BED)

CONTOUR INTERVAL 100 FEET — VELOCITY FEET PER SECOND
INTERPRETATION BY G.D. KNOWLES
DATUM: SEA LEVEL

LEGEND

- REFLECTION SHOT POINT (UNITED)
- OTHER SHOT POINTS
- REFRACTION SHOT POINT
- PERMANENT MARKER
- ASTROFIX
- TELLUROMETER STATION

MAP DATA

CONTROL: HORIZONTAL - BASIC FIRST ORDER CONTROL ESTABLISHED BY THE AUSTRALIAN DEPT. OF LANDS, TELLUROMETER TRAVERSE.
SECOND ORDER CONTROL PROVIDED BY CONTRACTORS TO PETROLEUM LTD. AND DEPT. OF LANDS, TELLUROMETER TRAVERSE.
THIRD ORDER CONTROL PROVIDED BY CONTRACTORS TO PETROLEUM LTD. ACCURACY HIGHER THAN 1 IN LENGTH OF TRAVERSE.
VERTICAL - C.A. DEPT. OF LANDS, LYOT AUTOMATIC LEVEL TRAVERSE, THIRD ORDER ACCURACY.
LOOP TRAVERSE - ACCURACY 0.05 FT (MAX.) LENGTH OF TRAVERSE IN MILES

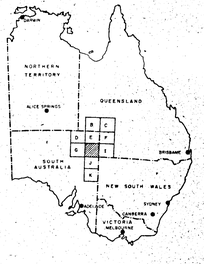

*TRANSVERSE MERCATOR PROJECTION

Figures from R.A.S.C. tables based on CLARKE'S 1858 SPHEROID
Compiled by J.R.Homer, senior draftsman Delhi Australian Petroleum Ltd.

SCALE 1:250,000
Statute Miles

SHEET "H"

Record No 1977/41

H.54/B13

1:250,000

PLATE 3

SOUTHERN COOPER BASIN SEISMIC SURVEY

BASE OF MESOZOIC

LEGEND

OTHER BOREHOLE

FAULT

ANTICLINE

SYNCLINE

PATCHAWARRA - EAST. - FLINDERS PET.

PATCHAWARRA - CENTRAL - BRIDGE OIL N.L.

MERRIMELIA - INNAMINCKA - SANTOS - AL. TANCO

PATCHAWARRA SOUTHWEST - PEXA - VAMGAS

MURTA - PEXA - VAMGAS

NOT AVAILABLE FOR FARMOUT

LAKE EYRE FARMOUT

ASHBURTON

TINGA TINGANA

PEXA-VAMGAS

MURTA PEXA VAMGAS

LAKE GREGORY

SOUTH AUSTRALIA

QUEENSLAND

N.S.W.

QLD.

S.A.

N.S.W.

NORTHERN TERRITORY

ALICE SPRINGS

BRISBANE

SYDNEY

MELBOURNE

TRANSVERSE MERCATOR PROJECTION

Figures from R.A.S.C. tables based on CLARKE'S 1858 SPHEROID

Compiled by J.R.Homer, senior draftsman, Delhi Australian Petroleum Ltd.

SCALE 1:250,000

Record No. 1977/41

SHEET "H"

H54/B13-4

1:250,000

SHEET "H"

PLATE 4

SOUTHERN COOPER BASIN
SEISMIC SURVEY
SOUTH AUSTRALIA

BASE OF EIDDEALPA
"P" HORIZON

LEGEND

- REFLECTION SHOT POINT
- OTHER SHOT POINTS
- REFRACTION SHOT POINT
- PERMANENT MARKER
- ASTRO
- TELLUROMETER STATION

MAP DATA

CONTROL: HORIZONTAL - BASIC FIRST ORDER CONTROL PROVIDED BY SOUTH AUSTRALIAN DEPT OF LANDS, TELLUROMETER SURVEY
SECOND ORDER CONTROL PROVIDED BY DELHI AUSTRALIAN PETROLEUM LTD AND DEPT OF MINERAL RESOURCES, QUEENSLAND
THIRD ORDER CONTROL PROVIDED BY CLOSED LOOP TRAVERSE
ACCURACY = 1/0.4√M (M = LENGTH OF TRAVERSE IN MILES)
VERTICAL - S.A. DEPT OF LANDS, TELLUROMETER TRAVERSED FROM SEA LEVEL TIES TO FIRST THIRD ORDER CONTROL PROVIDED BY SEISMOS
LOOP TRAVERSE ACCURACY = 0.1√M
(M = LENGTH OF TRAVERSE IN MILES)

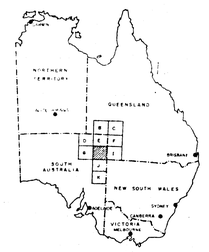

TRANSVERSE MERCATOR PROJECTION

Figures from R.A.S.C. tables based on CLARKE'S 1858 SPHEROID
Compiled by J.R.Homer, senior draftsman Delhi Australian Petroleum Ltd.

SCALE 1:250,000

Kilometres
Statute Miles

LAKE GREGORY

SOUTH AUSTRALIA
QUEENSLAND
N.S.W.
QLD.
S.A.
N.S.W.

Record No 1977/41

H 54/B13-25